Spatial and temporal dynamics of suspended sediment concentrations in coastal waters of South China Sea, off Sarawak, Borneo: Ocean colour remote sensing observations and analysis

Jenny Choo[1], Nagur Cherukuru[2], Eric Lehmann[2], Matt Paget[2], Aazani Mujahid[3], Patrick Martin[4], Moritz Müller[1]

[1]Swinburne University of Technology, Faculty of Engineering, Computing and Science, Jalan Simpang Tiga, 93350 Kuching, Sarawak, Malaysia.
[2]Commenwealth Scientific and Industrial Research Organization (CSIRO), Canberra ACT 2601, Australia.
[3]Faculty of Resource Science & Technology, University Malaysia Sarawak, Kota Samarahan 94300, Sarawak, Malaysia.
[4]Asian School of the Environment, Nanyang Technological University, 639798, Singapore.

Correspondence to: Jenny Choo (JChoo@swinburne.edu.my/jccy89@gmail.com)

Abstract

High-quality ocean colour observations are increasingly accessible to support various monitoring and research activities for water quality measurements. In this paper, we present a newly developed regional total suspended solids (TSS) empirical model using MODIS-Aqua's Rrs(530) and Rrs(666) reflectance bands to investigate the spatial and temporal variation of TSS dynamics along the southwest coast of Sarawak, Borneo. The performance of this TSS retrieval model was evaluated using error metrics (bias = 1.0, MAE = 1.47, and RMSE = 0.22 in mg/L) with a log10 transformation prior to calculation, as well as a k-fold cross validation technique. The temporally averaged map of TSS distribution, using daily MODIS-Aqua satellite datasets from 2003 until 2019, revealed large TSS plumes detected particularly in the Lupar and Rajang coastal areas on a yearly basis. The average TSS concentration in these coastal waters was in the range of 15 – 20 mg/L. Moreover, the spatial map of TSS coefficient of variation (CV) indicated strong TSS variability (approximately 90 %) in the Samunsam-Sematan coastal areas, which could potentially impact nearby coral reef habitats in this region. Study on temporal TSS variation provide further evidence that monsoonal patterns drive the TSS release in these tropical water systems, with distinct and widespread TSS plume variations observed between the northeast and southwest monsoon periods. A map of relative TSS distribution anomalies revealed strong spatial TSS variations in the Samunsam-Sematan coastal areas, while 2010 recorded a major increase (approximately 100 %) and widespread TSS distribution with respect to the long-term mean. Furthermore, study on the contribution of river discharge to the TSS distribution showed a weak correlation across time at both the Lupar and Rajang river mouth points. The variability of TSS distribution across coastal river points was studied by investigating the variation of TSS pixels at three transect points, stretching from the river mouth into territorial and open water zones, for eight main rivers. Results showed a progressively decreasing pattern of nearly 50 % in relation to the distance from shore, with exceptions in the northeast regions of the study area. Essentially, our findings demonstrate that the TSS levels at the southwest coast of Sarawak are within local water quality standards, promoting various marine and socio-economic activities. This study presents the first observation of TSS distributions at Sarawak coastal systems with the application of remote sensing technologies, to enhance coastal sediment management strategies for the sustainable use of coastal waters and their resources.

Keywords: total suspended solids, band-ratio, monsoon, river discharge, Open Data Cube

1.0 Introduction

Total Suspended Solids (TSS) play an important role in the aquatic ecosystem as one of the primary water quality indicators of coastal and riverine systems (Alcântara et al., 2016; Cao et al., 2018; Chen et al., 2015a; González Vilas et al., 2011; Mao et al., 2012). For example, elevated concentrations of TSS in water have an adverse impact on fisheries and biodiversity of the aquatic ecosystem (Bilotta and Brazier, 2008; Chapman et al., 2017; Henley et al., 2000; Wilber and Clarke, 2001). Understanding the impacts of varying water quality in relation to TSS status has been one of the primary concerns with respect to a country's growing Blue Economy status and sustainable management of aquatic resources (Lee et al., 2020a; Sandifer et al., 2021; World Bank and United Nations Department of Economic and Social Affairs (UNDESA), 2017). With about 40 % of the world's population living within 100 km of coastal areas (United Nations, 2017), and with more than 80 % of the population in Malaysia living within 50 km of the coast (Praveena et al., 2012), water quality monitoring and management efforts are important at both regional and global scale.

Studying TSS distribution can provide insights into the connections between land and ocean ecosystems (Howarth, 2008; Lemley et al., 2019; Lu et al., 2018). For instance, TSS dynamics allow us to understand the impacts of sediment transport and sediment plumes, particularly in areas experiencing large-scale deforestation, land conversion and damming of rivers (Chen et al., 2007; Espinoza Villar et al., 2013). Sarawak, Malaysian Borneo, experienced significant land use and land cover change activities over the past four decades, with widespread land conversion and deforestation for developments and large-scale plantation activities (Gaveau et al., 2016), as well as building of major road infrastructures, such as the Pan-Borneo highway, and hydroelectric dams (Alamgir et al., 2020). As a result, river and coastal systems may potentially drive large TSS loads into downstream systems and into the marine and open ocean waters.

Situated at the southern part of the South China Sea, the region of Sarawak, Malaysian Borneo, has a coastline of about 1035 km where mangrove forests are dominant (Long, 2014). The

coastal regions of Sarawak are rich with marine coastal biodiversity and coral reefs, which can be found at the northeast and southwest part of Sarawak (Praveena et al., 2012). While the coasts of Sarawak provide important socio-economic values to the local communities (Lee et al., 2020b), these coastal areas are potentially facing water quality degradation from TSS riverine outputs in response to land use and land cover change activities.

TSS concentrations are commonly measured through conventional laboratory-based methods to quantify TSS concentrations by field collection of water samples (Ling et al., 2016; Mohammad Razi et al., 2021; Soo et al., 2017; Soum et al., 2021; Tromboni et al., 2021; Zhang et al., 2013). Currently, real-time high-frequency TSS observations using modern optical and bio-sensor systems are also possible (Bhardwaj et al., 2015; Horsburgh et al., 2010). These sensors can be generally found onboard ship and buoy-based observation platforms. Yet, it remains a challenge to quantify TSS concentrations of large spatial coverage and high temporal frequency with these approaches.

Ocean colour remote sensing technologies represent an increasingly accessible and powerful tool to provide a synoptic view for short or long-term water quality studies at high temporal and spatial resolutions (Cherukuru et al., 2016a; Slonecker et al., 2016; Swain and Sahoo, 2017; Wang et al., 2017; Werdell et al., 2018). Remote sensing can help overcome several constraints of conventional intensive field campaigns such as: (i) costly field campaigns from boat rentals or cruise; (ii) time-consuming and inadequate manpower; and most importantly for this study, (iii) limited spatial and temporal field coverage. NASA's Moderate Resolution Imaging Spectroradiometer (MODIS)-Aqua (https://modis.gsfc.nasa.gov/about/) has a distinctive advantage with its daily revisit time, a spatial resolution of 250 – 1000 m, and a large collection of ocean colour data since 2002. Other sensors offering ocean colour measurement capabilities include Landsat-8, which, in comparison with MODIS-Aqua, has a 16-day revisit time and high spatial resolution of 30 m. Despite Landsat's powerful ability in capturing higher resolution images, the longer revisit interval may not be suitable for characterizing and studying water bodies with high dynamics of various water constituents.

Several MODIS-derived models have been developed for TSS retrievals (Chen et al., 2015b; Espinoza Villar et al., 2013; Jiang and Liu, 2011; Kim et al., 2017; Zhang et al., 2010b), including empirical, semi-analytical and machine-learning approaches (Balasubramanian et al., 2020; Jiang et al., 2021). However, the performance of these models proved to be less satisfactory, with recorded low r^2 and high bias and mean absolute error (MAE) values when tested with in situ TSS datasets (Supplementary Materials, Table S1). While these global TSS remote sensing models address the need to improve TSS retrievals and to monitor global TSS trends in various water class types, they tend to underperform in more localised and regional studies (Mao et al., 2012; Ondrusek et al., 2012). The coastal waters of Borneo are well-mixed throughout the year and enriched with suspended material and dissolved organic matter (Müller et al., 2016). Various water quality studies of the river systems have been actively carried out to assess the dynamics of numerous water quality constituents in response to human activities, with TSS concentrations being one of the primary environmental concerns in this region (Ling et al., 2016; Müller-dum et al., 2019; Tawan et al., 2020). Although studies on the water quality of coastal systems in Borneo have gradually gained much attention (Cherukuru et al., 2021; Limcih et al., 2010; Martin et al., 2018; Soo et al., 2017), there is still much knowledge to gain on the understanding of how coastal waters in the region have been impacted by TSS loadings and transport over large spatial and temporal scales.

Here, in this paper, we present a new regional empirical TSS remote sensing model. While various remote sensing models have their own unique computational strengths, this study demonstrates the reliability of band ratio TSS model to be applied within optically complex waters. With the ongoing efforts to address and minimize water quality degradation in coastal systems, as outlined in the United Nation's Sustainability Development Goals no. 14, our study aims to apply the new empirical regional TSS remote sensing model to: (a) investigate the spatial and temporal variability in TSS, (b) identify hotspots of TSS distribution in the coastal waters of Sarawak, Malaysian Borneo, using a long time series of MODIS-Aqua data from year 2003 until 2019, and (c) study the varying monsoonal and river discharge patterns in relation to TSS distribution at river mouths.

2.0 Methodologies

Figure below summarizes the processes carried out in this study. Spatial and temporal variation of TSS distribution was mapped using atmospheric-corrected MODIS-Aqua Level 2 product.

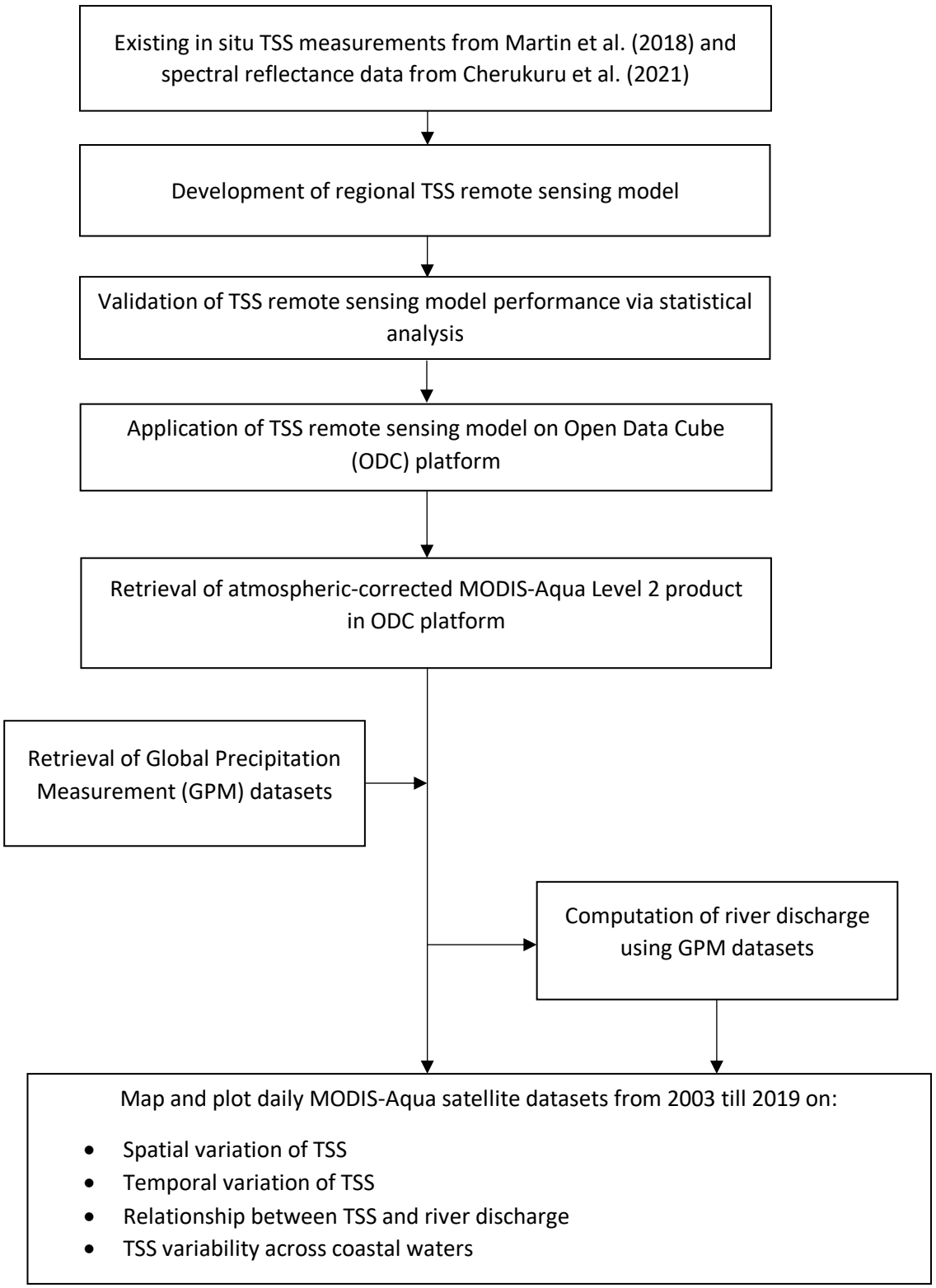

Fig. 1: Flowchart summarizing the processes of developing a regional TSS remote sensing model and applying it to analyse the spatial and temporal variation of TSS over the study region, using MODIS-Aqua data from year 2003 until 2019. Long-term MODIS-Aqua datasets were analysed and mapped on an Open Data Cube (ODC) platform with implementation of robust Python libraries and packages.

2.1 Area of study

Our study focuses on the southwestern coast of Sarawak (between 1.9° N, 109.65° E and 2.8° N, 111.5° E) in Malaysia, which sits at the northwest part of the Borneo Island. Generally, the island of Borneo (between 3.01° S, 112.18° E and 6.45° N, 117.04° E) contains rich tropical rainforests and biodiversity on the lands of Sarawak and Sabah (Malaysia), Brunei, and Indonesia. Typically, Sarawak is a tropical climate region, recording an average ambient temperature of 27.8 °C (variation of 1.8 °C) throughout the year. It records high precipitation with an average of 4116.7 mm/yr in Kuching (1.5535° N, 110.3593° E), the capital city of Sarawak. Yearly, it experiences both a dry and wet season, which is influenced by: (i) the southwestern monsoon (May to September) and (ii) the northeastern monsoon (November to March). Rivers in Sarawak are connected to the South China Sea and flow through various plantation types, such as oil palm, rubber and sago (Davies et al., 2010).

In this study, the southwestern part of Sarawak's coastal regions (Fig. 2), (between 1.9° N, 109.65° E and 2.8° N, 111.5° E) was studied, which comprise several major rivers (e.g. Lupar, Sebuyau, Sematan), as well as the Rajang River, the longest river in Malaysia. Rajang river basin consists in tidally influenced river channel which splits into a northwest (Igan, Lassa and Paloh) and a southwest (Rajang, Belawai) Rajang river delta (Staub et al., 2000). The Rajang river basin drains a dominant area (>50,000km^2) of sedimentary rocks (Milliman and Farnsworth, 2013; Staub et al., 2000) extending from Belaga to Sibu, with major peatland areas converted into oil palm plantations (Gaveau et al., 2016) as its river flows into the South China Sea (Milliman and Farnsworth, 2013). Major settlements along the Rajang river comprise of Kapit and Kanowit town areas, as well as Sibu city, with a total population size of about 388,000 inhabitants (Department of Statistics, 2020). Lupar and Saribas rivers, respectively, comprise a catchment area size of approximately 6500 and 1900 km^2 (Lehner et al., 2006). Situated at the southwest side of the Rajang catchment, Lupar and Saribas rivers surround the Maludam National

Park, which is Sarawak's remaining biggest single patch of peat swamp forest (Sarawak Forestry Corporation, 2022). Adjacent to Lupar river mouth is the Sadong river, with an approximate catchment area size of 3500 km^2 (Kuok et al., 2018). Sadong river runs about 150 km and flows through oil palm plantations (Staub and Esterle, 1993). These river systems are associated with increasing land use activities and land cover changes in this region, which essentially transport and connect various biogeochemical water components to the coastal systems of Sarawak.

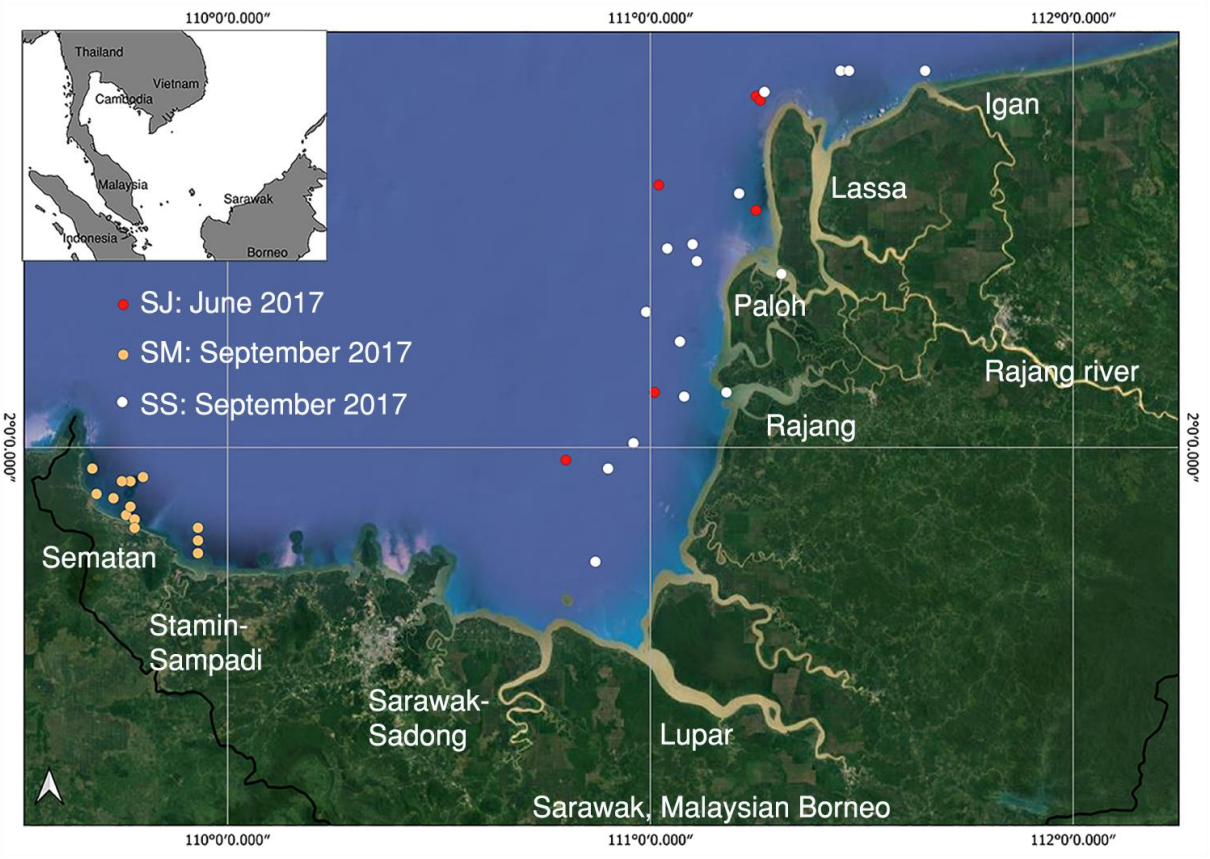

Fig. 2: Map of the study area (© Google Maps), located in the southwestern part of Sarawak, Malaysia (inset). Indicators show the location of sampling sites used during field expeditions carried out in June and September 2017.

2.2 In situ TSS measurements

TSS measurements were taken from Martin et al. (2018). A total of 35 coastal sites were studied and are denoted SJ, SS, and SM (see: Table 1 & Fig. 2). These water samples were collected in the month of June (SJ region) and September (SS and SM regions) in 2017. Water samples were filtered, and

185 filters were dried and ashed prior to weighing process. Full details of water sampling and TSS analysis
186 is available in Martin et al. (2018).

187 2.3 Development, calibration and validation of TSS model

188 In situ remote sensing reflectance spectral data, Rrs(λ), along with 35 measured TSS values, were used
189 to develop a new remote sensing TSS empirical model for MODIS-Aqua for this case study. Field
190 measurements of SM, SJ & SS datasets, as shown in Table 1, were used to calibrate the MODIS-Aqua
191 TSS remote sensing model.

192 For the in situ remote sensing reflectance, Rrs(λ) readings, a TriOS-RAMSES spectral imaging
193 radiometer was used to measure downwelling irradiance, Ed(λ), and upwelling radiance, Lu(λ), with
194 measurement protocols from Mueller et al. (2002). These measurements were recorded under stable
195 sky and sea conditions during the day (10AM to 4PM) with high solar elevation angles.

196 Measurements of reflectance, Rrs(λ), were recorded concurrently with the collection of water samples
197 (as described in Section 2.2) and were recorded at wavelength ranging from 280 to 950 nm, which
198 covers the spectrum of ultraviolet, visible and visible/ultraviolet light. These measurements were
199 recorded on a float to capture Lu(0−, λ) and Ed(0+, λ), where 0- and 0+ refer to below-surface and
200 above-surface, respectively.

201 Remote sensing reflectance, Rrs(λ), was computed as follows with reference to Mueller et al. (2002):

$$\mathrm{Rrs}(\lambda, 0+) = \frac{1-\mathrm{p}}{\mathrm{n}^2} \times \frac{\mathrm{Lu}(0-, \lambda)}{\mathrm{Ed}(0+, \lambda)} \qquad (1)$$

202 where p = 0.021 refers to the Fresnel reflectance and n =1.34 is the refractive index of water. Full
203 details of this methodology can be found at Cherukuru et al. (2021).

204 2.3.1 Calibration of empirical model and application to MODIS-Aqua

With the intention to apply a regional TSS remote sensing model to MODIS-Aqua product, a total of 35 different datasets of TSS concentrations were collected in coastal conditions (salinity > 15 PSU) and convolved to generate MODIS-Aqua data.

In this study, retrieval of water constituents was established using spectral band ratio combinations which have proven to be a straightforward, yet reliable method for estimating water constituents in optically turbid waters (Ahn and Shanmugam, 2007; Cao et al., 2018; Lavigne et al., 2021; Morel and Gentili, 2009; Neil et al., 2019; Siswanto et al., 2011). Band ratio models help to offset signal noise, such as the effects of atmospheric and irradiance of spectral reflectance to a certain degree (Cherukuru et al., 2016b; Ha et al., 2017; Hu et al., 2012; Liu et al., 2019).

A variety of models using single bands, as well as a combination of MODIS-Aqua's Blue, Green & Red bands (412nm, 440nm, 488nm, 532nm, 555nm & 660nm) were calibrated using field measurements as dependent variable. The calibration process was tested out using various model functions, including linear, power, exponential, and logarithm functions. The best empirical TSS retrieval model was fitted by means of a regression between the in situ TSS data and in situ radiometer values, and can be expressed as follows:

$$TSS = 21.238[Rrs(530)/Rrs(666)]^{-1.272} \quad (2)$$

This power function model resulted in a coefficient of determination (R^2) of 0.82 (Fig. 3).

Table 1: Summary statistics of TSS values collected at areas SJ, SS, and SM located within coastal regions in this study, with a total of 35 datasets recorded.

Coastal Area	Minimum	Maximum	Mean	S.D.	C.V.	n
SJ	1.1	19.24	6.89	6.62	96.09	6
SS	0.56	32.1	12.50	11.43	91.45	16
SM	0.5	8.14	2.59	2.70	104.53	13

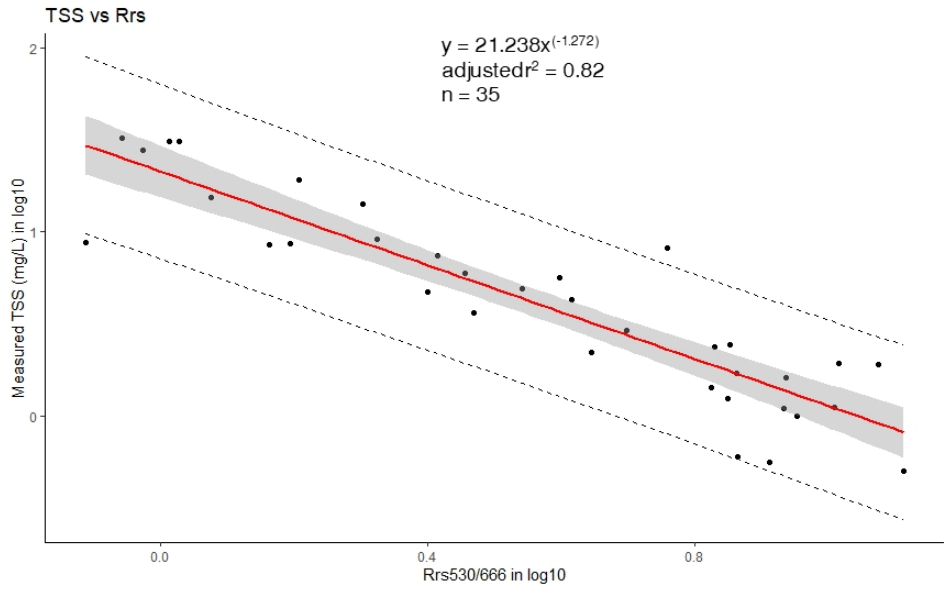

225

226 Fig. 3: Empirical relationship of TSS retrieval between in situ Rrs(530)/Rrs(666) bands ratio and measured TSS
227 concentration (mg/L), as established via a power law function. Upper and lower dashed lines indicate the 95 % prediction
228 interval of the regression.

229 2.3.2 Performance assessment and validation of MODIS-Aqua empirical model

230 An assessment of the performance error of the newly developed TSS model was carried out as per
231 Seegers et al. (2018)'s recommendation for interpreting ocean colour models. These performance
232 metrics used here include the bias, Mean Absolute Error (MAE), Root Mean Squared Error (RMSE),
233 coefficient of variation (CV), as well as the coefficient determination, r^2, based on the following
234 calculations:

235 $$\text{Bias} = 10^{\wedge}\left[\frac{\sum_{i=1}^{n} log10\,(Mi) - log10(Oi)}{n}\right] \quad (3)$$

236 $$\text{MAE} = 10^{\wedge}\left[\frac{\sum_{i=0}^{n} |\, log10\,(Mi) - log10(Oi)\,|}{n}\right] \quad (4)$$

237 $$\text{RMSE} = \sqrt{\frac{\sum_{i=1}^{n} (log10(Mi) - log10(Oi))^{\wedge}2}{n}} \quad (5)$$

238 $$\text{CV} = \frac{\sigma}{\mu} \text{ x } 100\% \quad (6)$$

239 where M represents the modelled TSS values, n is the number of samples, and O represents the
240 observed TSS measurements, while σ refers to standard deviation and μ represents the mean value.

241 Equations (3), (4) and (5) use a log10-transform of the data as the range of TSS values can span several
242 orders of magnitude. As such, an application of the log-transform prior to error metric calculation

allows us to account for uncertainties that are proportional to the concentration values (Balasubramanian et al., 2020; Seegers et al., 2018).

Table 2: Calibration and accuracy assessment of the newly derived MODIS-Aqua models in this study for TSS estimations tested using various model functions. Calculation for bias, MAE and RMSE use a log-transform of the data prior to calculation of error metric measurements, as adapted from Seegers et al. (2018) and Balasubramanian et al. (2020). Band ratio Rrs(530)/Rrs(666) is established as function x. Power function model is selected based on low performance metric values.

Model	Function	Bias	MAE	RMSE	CV (%)	R
Power	TSS = 21.238x^-1.272	0.9999	1.4732	0.2161	4.74	0.84
Linear	TSS = -1.8193x + 16.928	1.4463	1.8549	6.7174	20.699	0.6854
Exponential	TSS = 17.784e^-0.296x	1.0791	1.4906	6.3088	3.8920	0.8154
Logarithmic	-8.872ln(x)+19.383	1.1336	1.6177	5.3735	-17.056	0.8128

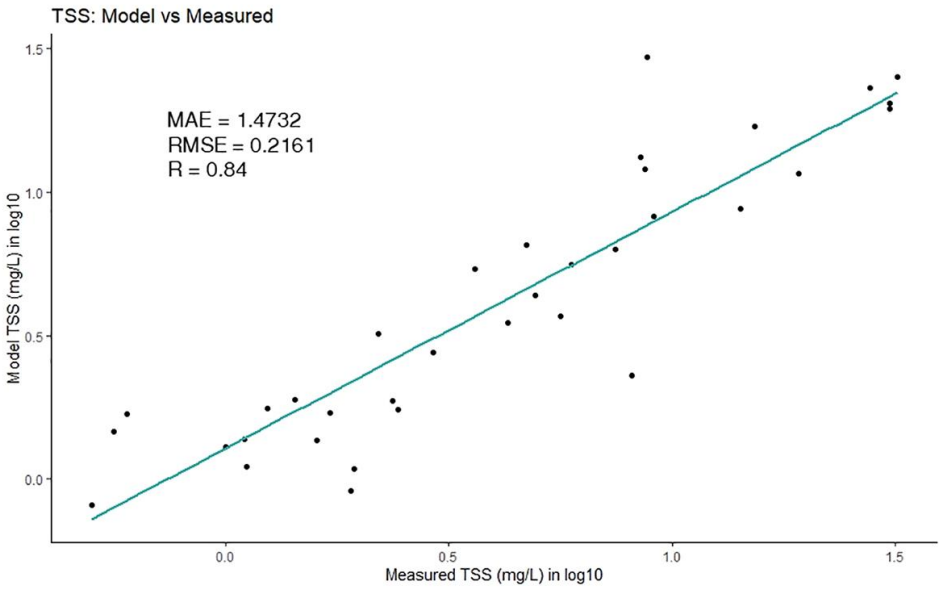

Fig. 4: Scatterplot of modelled TSS values derived from the proposed model and measured TSS values (mg/L).

An evaluation of the model was performed using a k-fold cross validation technique (Refaeilzadeh et al., 2020) given the small size of the TSS dataset used in this study (Table 2). A selection of k = 7 was assigned to split the datasets into k groups with an equal number of data points.

Table 2: Assessment of fitting error for the proposed TSS model, using k-fold cross validation.

Parameter	k-fold (n)	R2	RMSE	MAE
TSS	7	0.85	0.2159	0.1747

While these results point to low error levels achieved by the proposed regional TSS retrieval model (Table 3, Fig. 4), caution should be used when applying it to various water types. Water type classification has been thoroughly described by Balasubramanian et al. (2020) where waters are classed into Type I (Blue-Green waters), Type II (Green waters), and Type III (Brown waters). Essentially, the Green-to-Red band ratio is optimised with these datasets corresponding to sediment-dominated and yellow-substance loaded water conditions. As highlighted by Morel & Belanger (2006), waters of this type do not have the same spectral characteristics as phytoplankton-rich waters (also known as Case 1 waters). In addition to the impact on water clarity, sediment particles (often red-brownish coloured) also tend to enhance the backscattering and absorption properties, especially at shorter wavelengths (Babin et al., 2003), while the additional presence of coloured dissolved matter (yellow substance) leads to strong absorption properties at short wavelengths. As the TSS retrieval model was developed from samples taken in waters that are bio-optically rich in suspended solids and dissolved organic matter, an application of this TSS model needs to be done cautiously when applying to other water types, particularly those with large concentration of phytoplankton.

2.4 Application of TSS retrieval model

Daily MODIS-Aqua satellite data from year 2003 to 2019 (total of 6192 individual time slices) were studied with a 2°x 2° spatial resolution (longitude: 109.38, 112.0; latitude: 1.22, 3.35) which covers the southwestern coastal region of Sarawak and southern part of the South China Sea. Atmospherically corrected MODIS-Aqua level 2 reflectance products (Bailey et al., 2010; NASA Official,

n.d.) were retrieved for the application of the TSS model proposed in this study. Negative remote sensing reflectance values, possibly due to failure of atmospheric correction, were filtered out before applying the retrieval model, as expressed in Eq. (2), to map the spatial and temporal distribution of TSS estimates. In addition, averaging of spatial and temporal TSS variation maps in this study was carried out by filtering TSS values with fewer than 10 valid data points over the whole time series, along with application of sigma clipping operation (refer to: https://docs.astropy.org/en/stable/api/astropy.stats.sigma_clip.html).

2.4.1 Open Data Cube

In this study, the analysis of remote sensing data over large spatial extents and at high temporal resolution was carried out using robust Python libraries and packages run on an Open Data Cube (ODC) platform. Open Data Cube is an open-source advancement in computing technologies and data architectures which addresses the growing volume of freely available Earth Observation (EO) satellite products (Giuliani et al., 2020; Killough, 2019). ODC provides a collection of software which index, manage, and process large EO datasets such as satellite products from the MODIS, Landsat and Sentinel missions (Gomes et al., 2021). These satellite datasets are structured in a multi-dimensional array format, and provide layers of information across latitude and longitude (Open Data Cube, 2021). Leveraging the growing availability of Analysis Ready Data (ARD), and with support from the Committee of Earth Observation Satellites (CEOS) (Killough, 2019), the ODC concept has been deployed in many countries across the world. These existing deployments include Digital Earth Africa (https://www.digitalearthafrica.org/), Digital Earth Australia (DEA) (https://www.dea.ga.gov.au/), Vietnam Open Data Cube (http://datacube.vn/), and Brazil Data Cube (https://github.com/brazil-data-cube), which provide various time-series datasets of the changing landscape and water content in these specific regions (Giuliani et al., 2020; Gomes et al., 2021; Killough, 2019; Lewis et al., 2017). The ecosystem and architecture of ODC is well explained at opendatacube.org. The codes and tools used

in this application drew upon the information provided in various DEA notebooks (Krause et al. (2021), which can be found at https://github.com/GeoscienceAustralia/dea-notebooks/.

2.5 Precipitation data and computation of river discharge

Monthly precipitation values (mm) over the Lupar and Rajang basins were extracted from the Global Precipitation Measurement (GPM) Level 3 IMERG satellite datasets (https://gpm.nasa.gov/data/imerg) in order to assess the influence of precipitation in each river basin in relation to TSS concentration at the corresponding river mouth (Supplementary Materails, Fig. S4 – 7).

Derivation of river discharge (m^3/s) was computed using total precipitation estimates (mm) over each river basin, and multiplied by a surface discharge runoff factor for the studied region (Sim et al., 2020). The surface runoff was estimated to be 60 % of total precipitation (Staub et al., 2000; Whitmore, 1984). In this study, the Rajang river basin, as well as the combined basins of the Lupar, Sadong, and Saribas rivers (hereafter referred to as the Lupar basin), were studied for their river discharge rates in relation to TSS release.

3.0 Results & Discussion

3.1 Spatial variation of TSS distribution

Changes in TSS distribution occur across space and time. The regional TSS remote sensing model calibrated in this study was applied to the time series of MODIS-Aqua data to study the variability of spatial TSS distribution and identify potential hotspot areas susceptible to TSS water quality degradation. The map of average TSS for the Sarawak region was generated (Eq. 2) by averaging all the daily MODIS-Aqua TSS images (2003 to 2019) and is presented in Fig. 5. The results show that the waters in the northeast region of the study area, stretching from the Sadong river to the Rajang/Igan river have seen sustained levels of TSS over the 17 years considered in this study.

The temporally averaged spatial distribution map (Fig. 5) shows TSS concentrations in the range of 15 – 20 mg/L near the river mouth areas, with widespread TSS plumes extending into the South China Sea (Fig. 5). Based on the Malaysia Marine Water Quality Criteria and Standard (Supplementary Materials, Table S2) (Department of Environment, 2019), these coastal waters fall under Class 1 in relation to their TSS (mg/L) status. This classification indicates that these coastal waters support and preserve marine life in this local region. Yet, several studies have expressed concerns regarding high TSS loadings in riverine waters owing to the impacts of various land use and land cover changes (LULC) (Ling et al., 2016; Tawan et al., 2020). Among these, the Rajang river has been highlighted to be heavily impacted by various LULC activities such as large-scale deforestation and construction of hydropower dams (Alamgir et al., 2020). In situ water quality studies by Ling et al. (2016) reported on high TSS estimates at one of the upstream tributaries of Rajang river, the Baleh river, with TSS readings up to approximately 100 mg/L. Another study by Tawan et al. (2020) reported a significant TSS release reaching to 940,000 mg per day during wet seasons, with maximum TSS concentrations of 1700 mg/L in the upstream tributaries of the Rajang river, particularly at the Baleh and Pelagus rivers. The majority of the upstream tributary rivers were categorised as Class II (during dry season) and Class III (during wet season) waters according to the National Water Quality Index (Supplementary Materials, Table S3) (Department of Environment, 2014), due to increased soil erosion from surrounding LULC activities (Tawan et al., 2020). These local in situ findings provide valuable insights on point source TSS estimates in these LULC change regions. Coupled with our spatial map of average TSS captured by remote sensing technologies, our findings seem to suggest that a large portion of TSS loadings from inland and upstream rivers would have settled and deposited in these river channels and were not completely discharged outwards into the coastal areas, which would have caused major water quality degradation in the corresponding coastal systems.

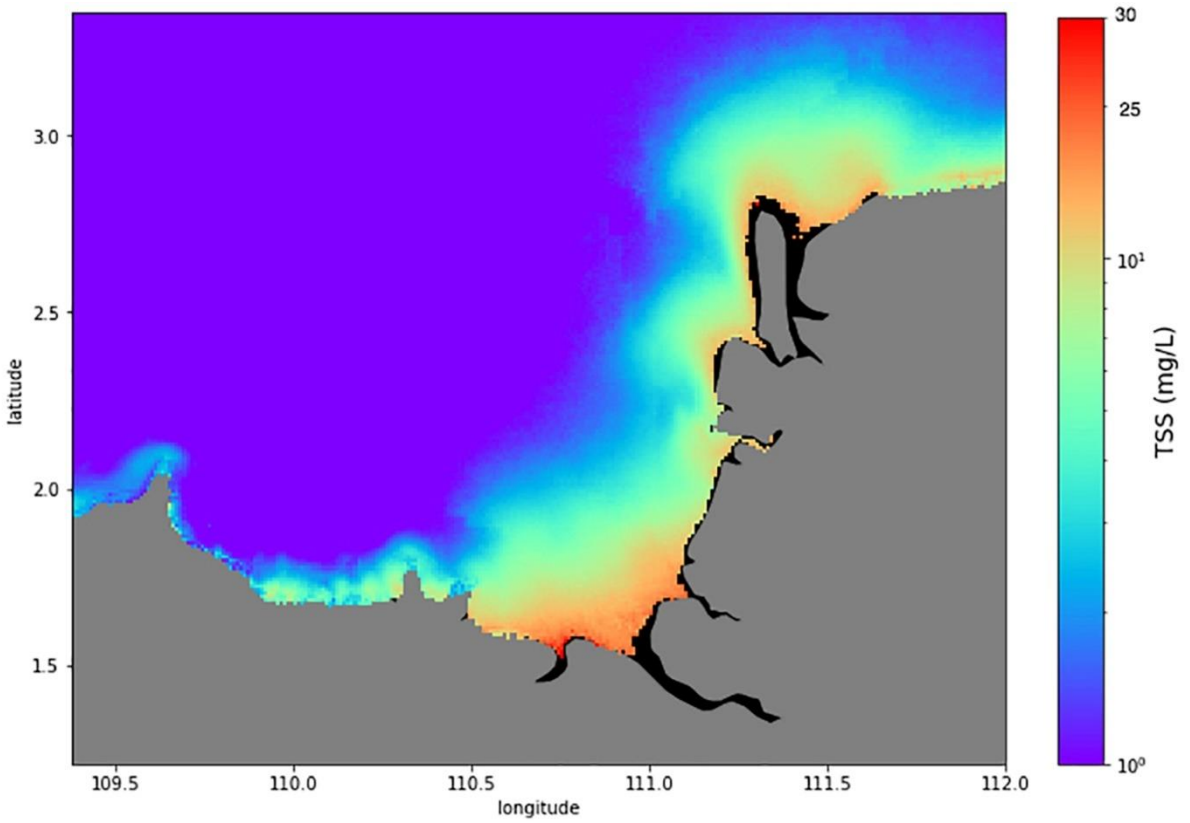

Fig. 5: Temporally averaged 2°x 2° map of TSS distribution (on a log scale) across the time dimension for each pixel.

Historical patterns of TSS concentration were assessed by comparing annual maps of average TSS distribution (Supplementary Materials; Fig. S1), as well as time series of TSS estimates at the Lupar and Rajang river mouths (Supplementay materials; Fig. S2). From our findings, the annual TSS maps further support the observation where TSS release was evident at Lupar and Rajang/Igan river mouths from 2003 till 2019, which points to Class I of local water quality standards in relation to TSS (mg/L) status. This was found to consistently occur every year. Furthermore, the TSS trend study showed that both the Lupar and Rajang river mouth points have a gradual increase of TSS concentration over the 17 years (Supplementay materials; Fig. S2). This increasing trend was, however, not statistically significant ($p = 0.43$ for Lupar, and $p = 0.15$ for Rajang).

Moreover, a map of the TSS coefficient of variation (CV) was computed to identify areas with a high degree of relative TSS variation over time (Fig. 6). Here again, the map of CV (%) was produced by aggregation of the daily MODIS-Aqua images (6192 time steps) from 2003 until 2019. Figure 6 shows

362 that the Samunsam-Sematan coastal region (as highlighted by the red box) exhibits an increased level
363 of TSS distribution variability, with a recorded CV of more than 90 %.

364 The Samunsam-Sematan coastal region contains near-pristine mangrove forests which are sheltered
365 from major LULC activities, as compared to other studied sites. Samunsam-Sematan is also well-known
366 locally as a recreational hotspot with coral reefs and various national parks (Sarawak Tourism Board,
367 2021). Data from the Centre for International Forestry Research (CIFOR) Forrest Carbon database
368 (CIFOR, n.d.) revealed that there was more than double the amount of total forest loss (approx. 5,000
369 Ha) recorded in Lundu, a nearby township in the Sematan area in 2011 as compared to the previous
370 years. Deforestation activities, regardless of their scale, can inevitably promote sediment loss and soil
371 leaching into the nearby river systems (Yang et al., 2002). Important information regarding the
372 variability in water quality (as shown in Fig. 6) can provide support to local authorities and relevant
373 agencies in order to identify vulnerable areas that need to be monitored closely, such as the Lundu-
374 Sematan region in this case. The CV map thus offers interesting insights into how TSS distribution can
375 vary across large spatial areas, which can ultimately impact local socio-economic activities in this
376 region (Lee et al., 2020b).

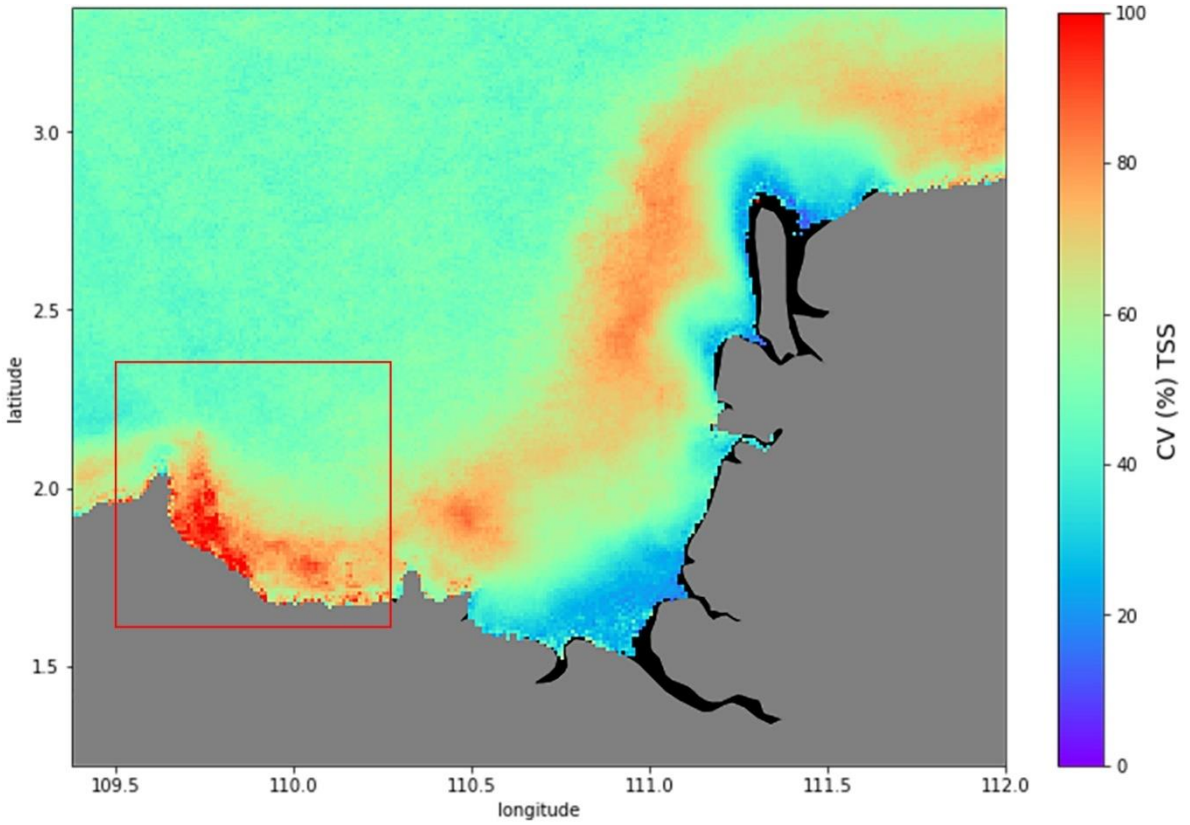

377

378 Fig. 6: Map of CV (%) calculated from the daily time series of MODIS-Aqua satellite images from 2003 until 2019.

379 3.2 Temporal variation of TSS distribution

380 On a temporal scale, the northeast (NE) monsoon period shows a distinct difference in the widespread
381 intensity of TSS distribution as compared to the southwest (SW) monsoon period, along the Sarawak
382 coastline over the 17 years of the considered time series (Fig. 7). Mapping of temporal variations
383 between monsoons using time-series MODIS-Aqua datasets can provide an improved understanding
384 on the intensity of monsoonal patterns in driving the TSS distribution in this region. As shown in Figure
385 7, TSS release can be seen to extend further into the open ocean South China Sea region during the
386 NE monsoon periods (Fig. 7a) in comparison to the SW monsoon periods (Fig. 7b).

387 In addition, the differences in TSS release between the NE and SW monsoons ((NE-SW)/NE x 100) were
388 mapped as shown in Fig. 7c. Widespread TSS plumes are detected at Lundu/Sematan region (>80 %
389 relative difference in TSS concentration) on the southwest side of the study area, while substantial
390 TSS plumes are observed in front of the Igan river channel, with more than 50 % relative difference in

391 TSS concentration in comparison to SW monsoon periods. Sadong coastal area is observed to receive
392 considerable TSS loadings (> 30%) during NE monsoon periods.

393 These coastal areas would thus be more likely to be impacted by the TSS release during the NE
394 monsoon periods. These findings further strengthen the evidence that tropical rivers are majorly
395 impacted by climatic variability such as monsoonal patterns, as highlighted in a study at Baleh river in
396 Sarawak (Chong et al., 2021). This suggests that monsoon rains, which typically last for several months,
397 play an integral role in driving the discharge of TSS in tropical rivers.

398

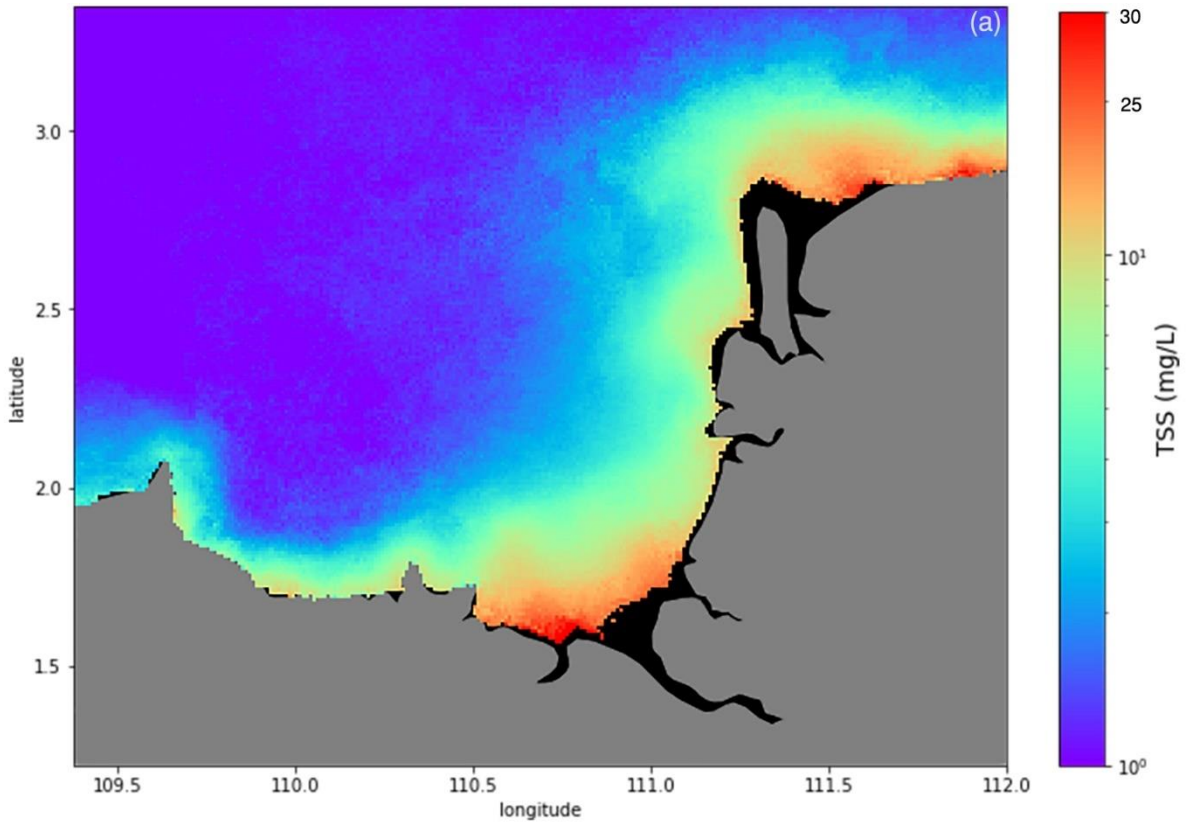

399

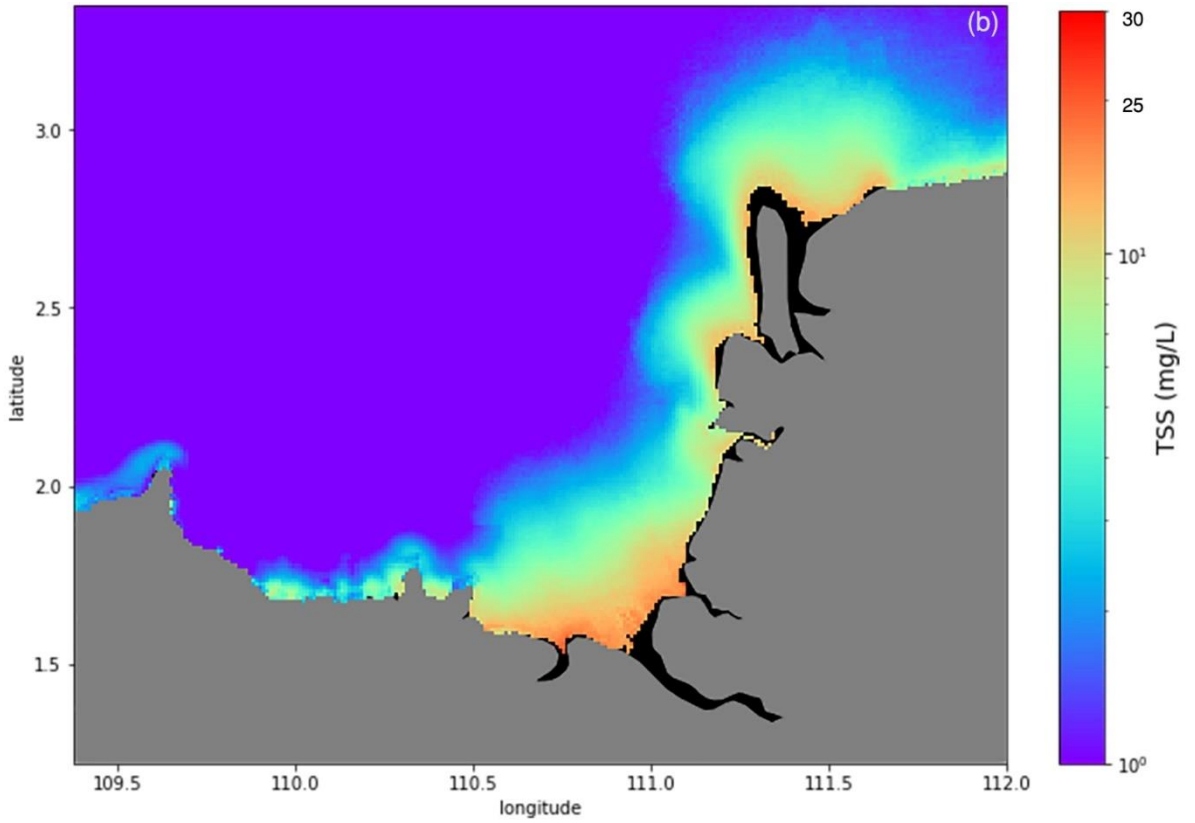

400

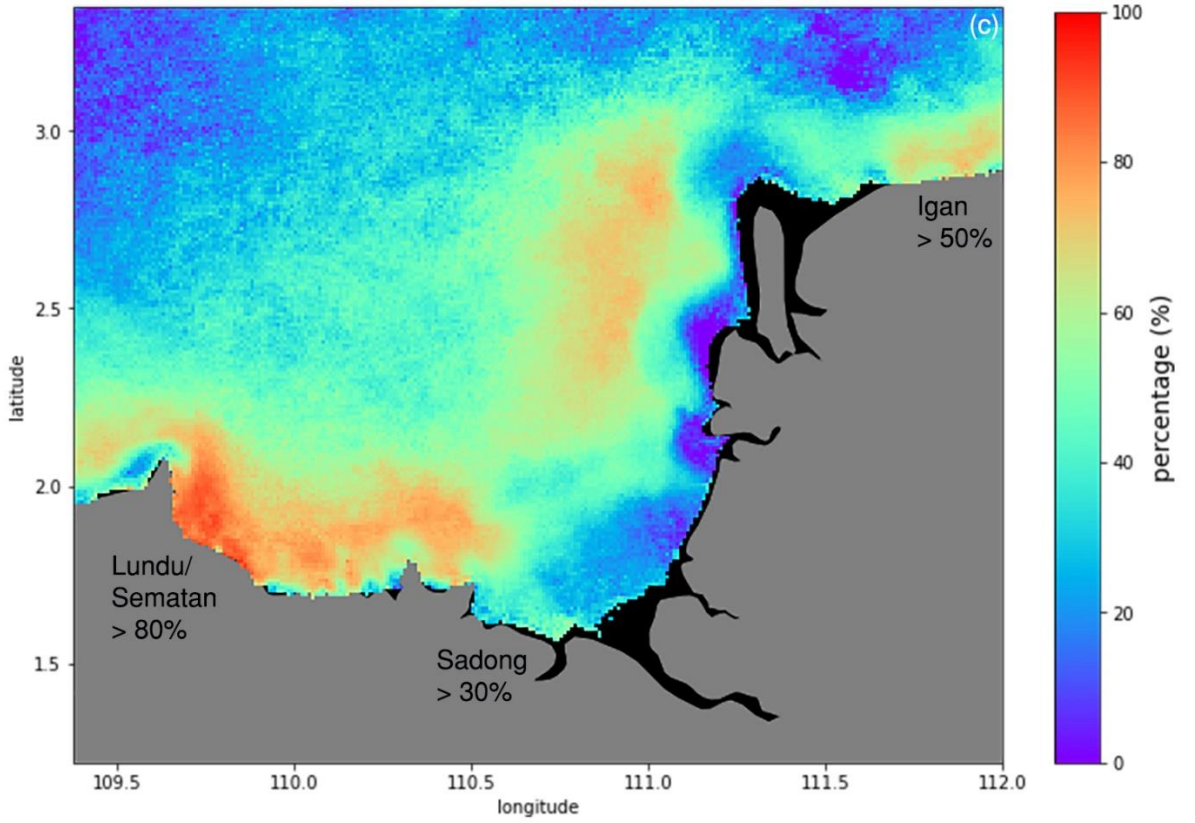

401

402 Fig. 7: Long-term average of TSS estimates (mg/L) during the Northeast monsoon (a), and the Southwest monsoon (b). The

map of TSS difference between the Northeast and Southwest monsoon periods, computed in relative percentage (%), is shown in (c).

Several climatic studies in the Borneo region highlighted 2009 as a year with extreme rainfall events which caused major floods in Sarawak (Dindang et al., 2011; Sa'adi et al., 2017), while drought events were reported in 2014 (Bong and Richard, 2020). Hence, in this study, TSS dynamics for the Lupar and Rajang rivers were studied by assessing the variation of TSS values at selected pixels in relation to monsoonal rainfall patterns in 2009 and 2014 (Supplementary Materials; Fig. S3).

Generally, the results show fluctuations of TSS concentrations across the NE and SW monsoon periods in relation to precipitation values (Fig. 8a – d). Based on Fig. 8a, monthly precipitation values recorded for the Lupar river basin in 2009 showed a clear decreasing trend from the NE monsoon period (wet season) to the SW monsoon period (dry season), while gradually increasing approaching the year end's NE monsoonal period. A similar precipitation pattern was observed for the Rajang river basin during the same year (Fig. 8c).

However, these results also show that the TSS distribution (mg/L) at the Lupar river mouth seems to show no distinct trend of decreasing TSS concentration estimates during the SW monsoon period in year 2009 (Fig. 8a) in relation to its precipitation values. Additionally, a sharp rise of TSS release can be seen in the month of May (beginning of SW monsoon period), with a near equivalent intensity of TSS release during the NE monsoon period. This observation may potentially be caused by the lag between the time of rainfall events occurring during NE monsoon periods and TSS release entering the coastal river regions. A similar observation was described by Sun et al. (2017a) suggesting that riverine outputs could take several days, and even up to one month to reach the coastal river points. Considering the occurrence of extreme rainfall events in 2009, our findings are in agreement with these processes as TSS concentrations generally exhibit a similar intensity throughout the NE and SW monsoonal periods for the Lupar river (Fig. 8a). This result could suggest that the occurrence of

extreme rainfall events, as reported for the year 2009, can exert a much larger impact on TSS transportation and release in monsoon-driven tropical rivers.

Drought events in 2014 can be seen to impact the precipitation values at both the Lupar (Fig. 8b) and Rajang river basins (Fig. 8d). There is no apparent patterns of decreasing precipitation values during the shift of NE to SW monsoonal periods as compared to the year 2009, for either river basin. However, precipitation values were found to increase sharply during the year end NE monsoon period for both river basins. The TSS concentrations at the Lupar coastal river points were found to be the highest during the NE monsoon period earlier in January and February of 2014 (Fig. 8b). This may be due to the temporal lag in the transition of TSS discharge into the coastal systems arising from the prior months (November and December) in the previous year, when higher rainfall events were typically observed in this region (Gomyo and Koichiro, 2009; Tangang et al., 2012). The TSS distribution at both Lupar and Rajang coastal river points showed no distinct trend in relation to the precipitation values throughout a period of ten months until November 2014. These findings suggest that coastal areas in the Borneo region may not be experiencing critical water quality degradation during dry seasons.

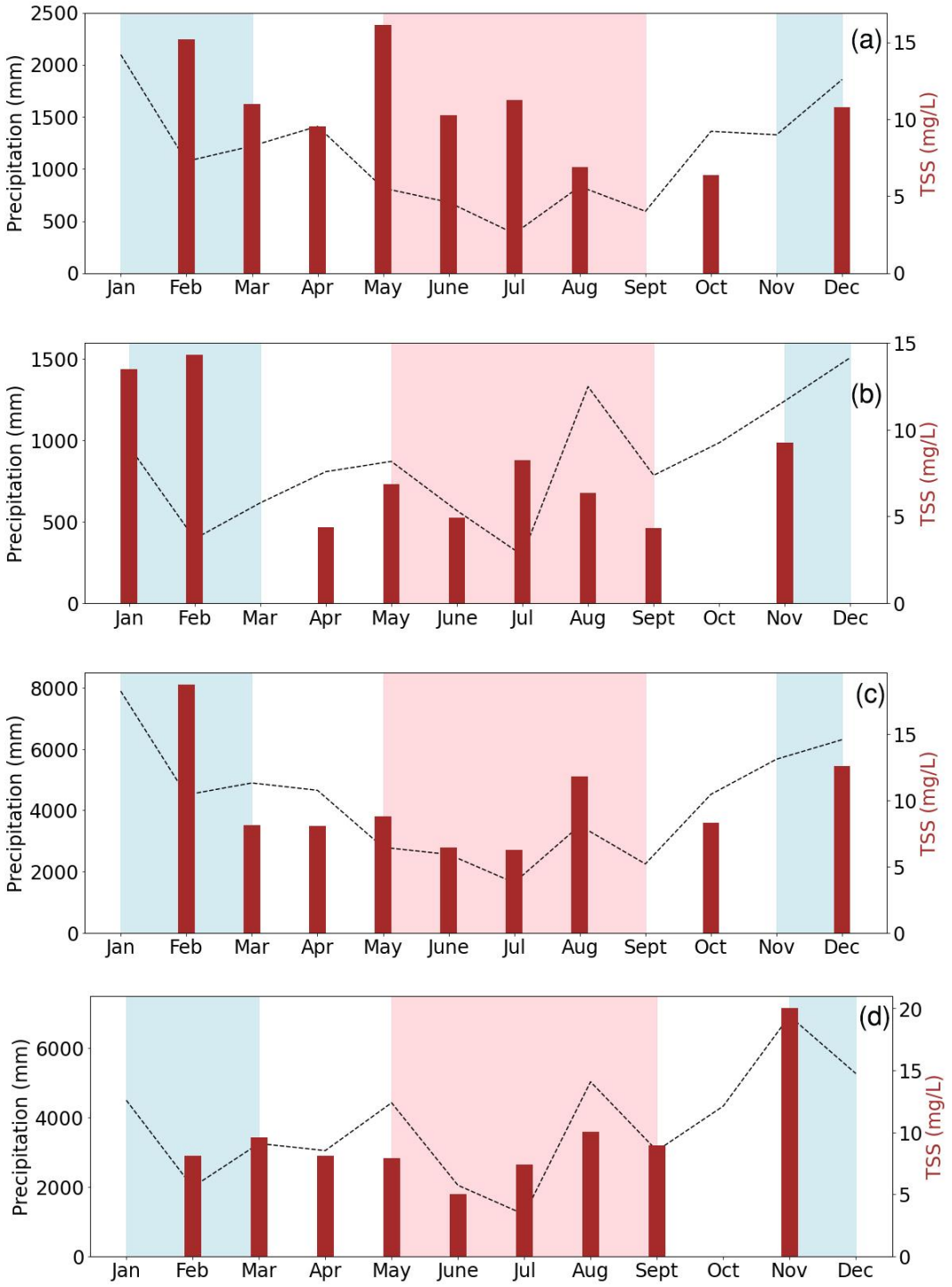

449

450 Fig. 8: Temporal analysis of precipitation (mm) from the Lupar and Rajang river basins in relation to TSS concentrations (mg/L)
451 during the NE and SW monsoon periods at the Lupar ((a): 2009; (c): 2014) and Rajang ((b): 2009; (d): 2014) coastal river point.
452 The NE monsoon months are highlighted with a blue background; those of the SW monsoon with a pink background, and
453 intermonsoon periods with a white background.

3.2.1 Temporal TSS anomalies

Considering the temporal variation recorded across monsoons, maps of relative TSS anomalies were calculated for each year as the difference with respect to the long-term TSS mean (Fig. 5), in order to detect changes of TSS distribution occurring annually (Fig. 9). As shown in Figure 9, year 2010 experienced a distinct increase of TSS distribution (approximately 100 %), with widespread pattern extending into open ocean waters, in comparison to the long-term TSS mean. This finding provides an interesting insight into the effects of extreme rainfall events as recorded in year 2009, which could potentially intensify TSS release into the coastal and open ocean waters. The effects of TSS release can still be seen a year after the extreme rainfall events in this region. This observation could provide further evidence that the impacts of the TSS release from the land into rivers and coastal systems may only take effect after a substantial period, as previously observed by Sun et al. (2017a).

Figure 9 further reveals an interesting pattern of TSS increase in the Samunsam-Sematan region from year 2004 until 2019, with exceptions during the years 2007 and 2008. As previously highlighted in Section 3.1, the Samunsam-Sematan region has been observed to be a vulnerable coastal area with respect to TSS water quality degradation. From the annual map of TSS anomalies (Fig. 9), we can see that the TSS distribution has the tendency to accumulate in the Samunsam-Sematan region, as opposed to being distributed into the open ocean waters. This may be due to the geographical and hydrological characteristics of these coastal regions (Martin et al., 2018), as the TSS release may be sheltered from open ocean waters, and hence induce a higher TSS accumulation in these coastal regions.

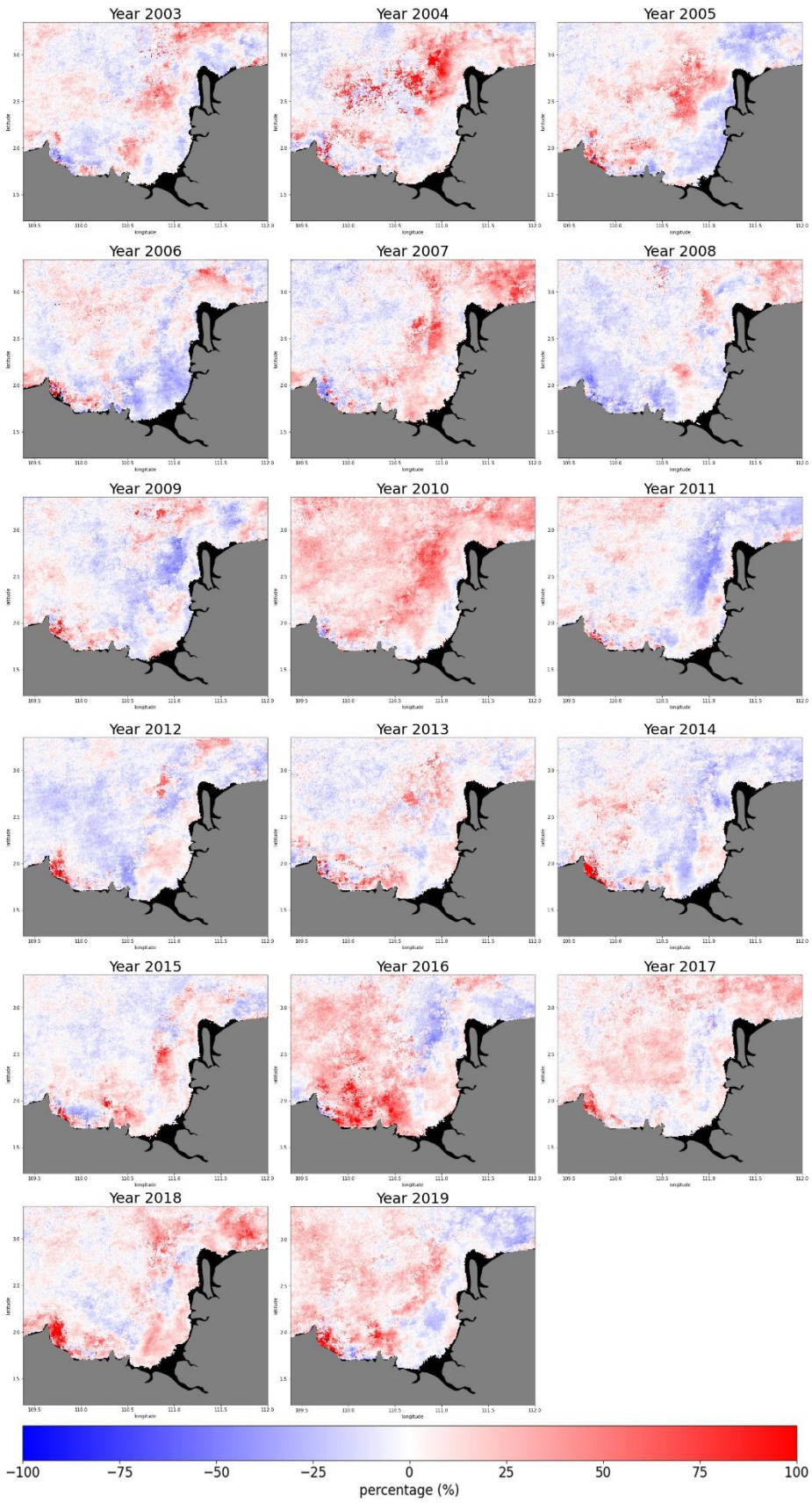

479

480 Fig. 9: Map of relative TSS distribution anomalies with respect to the long-term mean, represented as percentage (%), from

481 year 2003 until 2019.

3.3 Hydrological factors driving TSS discharge

Apart from the influence of monsoonal patterns, hydrological factors such as the river discharge are among the dominant drivers in transporting various water constituents in riverine and coastal systems (Loisel et al., 2014; Petus et al., 2014; Sun, 2017b; Verschelling et al., 2017). In this study, river discharge from the Lupar and Rajang basins was estimated and investigated.

Yearly river discharge estimates from 2003 until 2019 were investigated to assess its effect on the TSS distribution (Fig. 10) represented by changes in TSS values for pixels located at each Lupar and Rajang coastal river points (Supplementary Materials, Fig. S3). Figure 10a shows that river discharge values in the Lupar basin (750 to 1050 m^3/s) are approximately twice lower than the Rajang river discharge (Fig. 10b), which recorded a range of 3,200 to 4,000 m^3/s.

Fig. 10: Time-series analysis of river discharge (m^3/s) in relation to TSS concentrations (mg/L) for the Lupar (a) and Rajang (b) basins from year 2003 to 2019. Note the differing scaling on the ordinate axes in each plot.

Discrepancies between TSS estimates and river discharge were identified in both the Lupar and Rajang coastal regions in these annual time-series, where river discharge was inversely correlated with TSS estimates. These discrepancies are not uncommon, as previously highlighted in a study by Zhan et al. (2019). Especially in 2010 for the Lupar river, Fig. 10a shows a drop in TSS release in relation to the steady increase of river discharge from the river basin. In 2011 and 2012, a negative correlation can be seen between river discharge and TSS estimates, while in subsequent years from 2013 until 2015, there is a clear positive correlation. Although there is no obvious environmental factor that would explain these discrepancies, these findings may imply a complex interaction between human interventions, such as damming and deforestation activities, as well as varying hydrological and atmospheric conditions (wind and tidal mixing) in regulating TSS dynamics (Wu et al., 2012; Zhan et al., 2019).

The correlation between TSS release and river discharge at both the Lupar and Rajang coastal areas was further evaluated in this study. Even though river discharge has been shown (in other global studies) to be one of the dominant factors in moderating TSS release (Fabricius et al., 2016; Tilburg et al., 2015; Verschelling et al., 2017; Wu et al., 2012), the TSS distribution at both the Lupar and Rajang river mouths in this study can be seen to be only poorly correlated with river discharge from each river basin (Supplementary Materials, Fig. S8a and b). The TSS output from the Lupar basin recorded a correlation coefficient of $r = 0.15$, while river discharge from the Rajang basin did not substantially influence the TSS release either, with $r = 0.27$ throughout the seasons. Coupled with tidal mixing processes (Ramaswamy et al., 2004; Zhou et al., 2020) , it is possible that human activities such as deforestation, logging, and construction of dams, which are largely occurring within the Rajang basin (Alamgir et al., 2020), are mainly driving TSS release and resuspension in this area. This indicates that although TSS release is regarded to be highly dependent on, and controlled by river discharge patterns, this interaction often represents an intricate process linked to local hydrodynamics process and socio-economic conditions (Espinoza Villar et al., 2013; Fabricius et al., 2016; Valerio et al., 2018; Zhan et al., 2019).

3.4 Variability of TSS across coastal waters

As previously observed in Fig. 5, varying river plumes of TSS were evidently detected within the coastal regions of the study area. Notably, coastal river plumes represent important factors driving the transport of water constituents and nutrients from coastlines to the open oceanic systems (Petus et al., 2014). To assess this and evaluate the water quality status in coastal zones, the spatial extent of TSS release was investigated along transects covering the territorial (12 nautical miles) and open water areas (24 nautical miles) of the Sarawak region (Fig. 11).

A total of eight coastal points were selected based on the main river mouths located in the southwest region of Sarawak. Transect points are positioned in a line starting at the coastal river points to examine the variations of TSS distribution across different water zones. Daily changes in TSS concentration for each pixel located in front of the river mouths were plotted from 2003 until 2019 (Fig. 12).

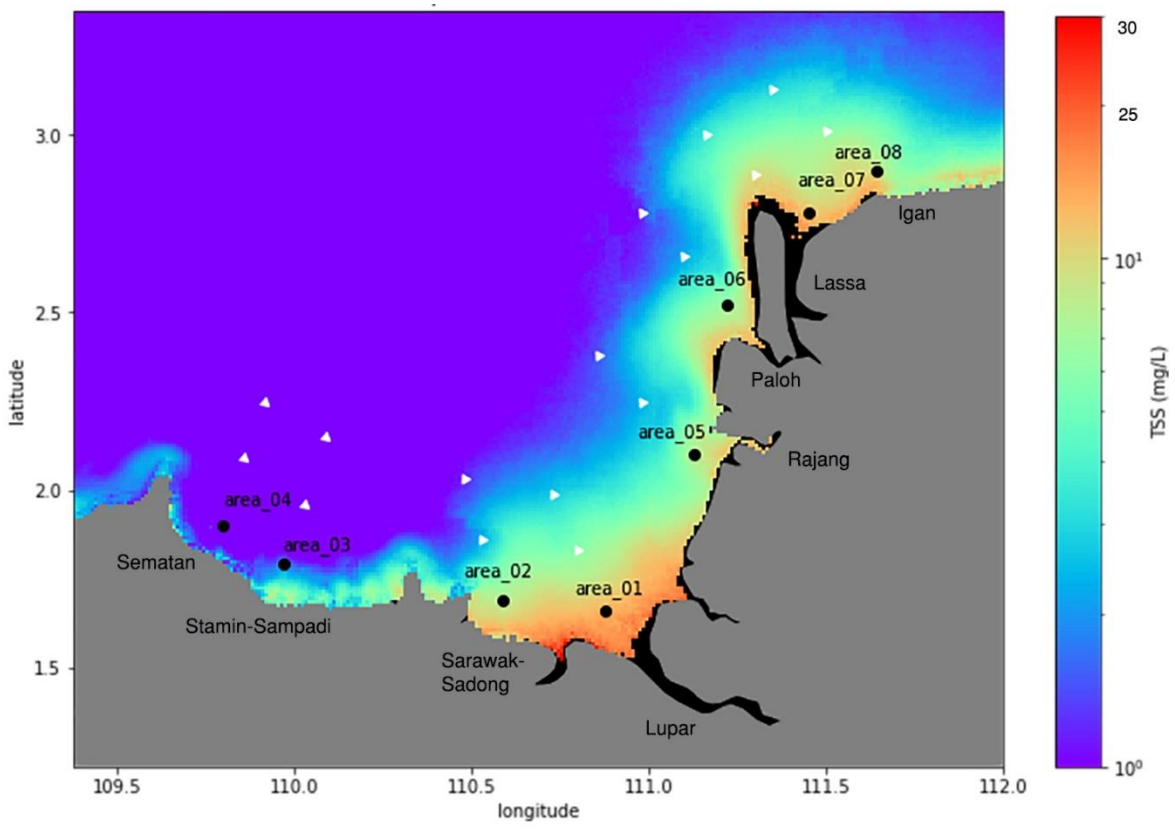

Fig. 11: Map of average TSS estimates (mg/L) with indicators at eight main river mouths and their transect, extending from coastal waters into territorial and open ocean systems. Indicators of each river mouths are as follows: area_01 – Lupar river; area_02 – Sarawak-Sadong river; area_03 - Stamin-Sampadi river i; area_04 – Sematan river; area_05: Rajang river; area_06: Paloh river; area_07: Lassa river; and area_08: Igan river).

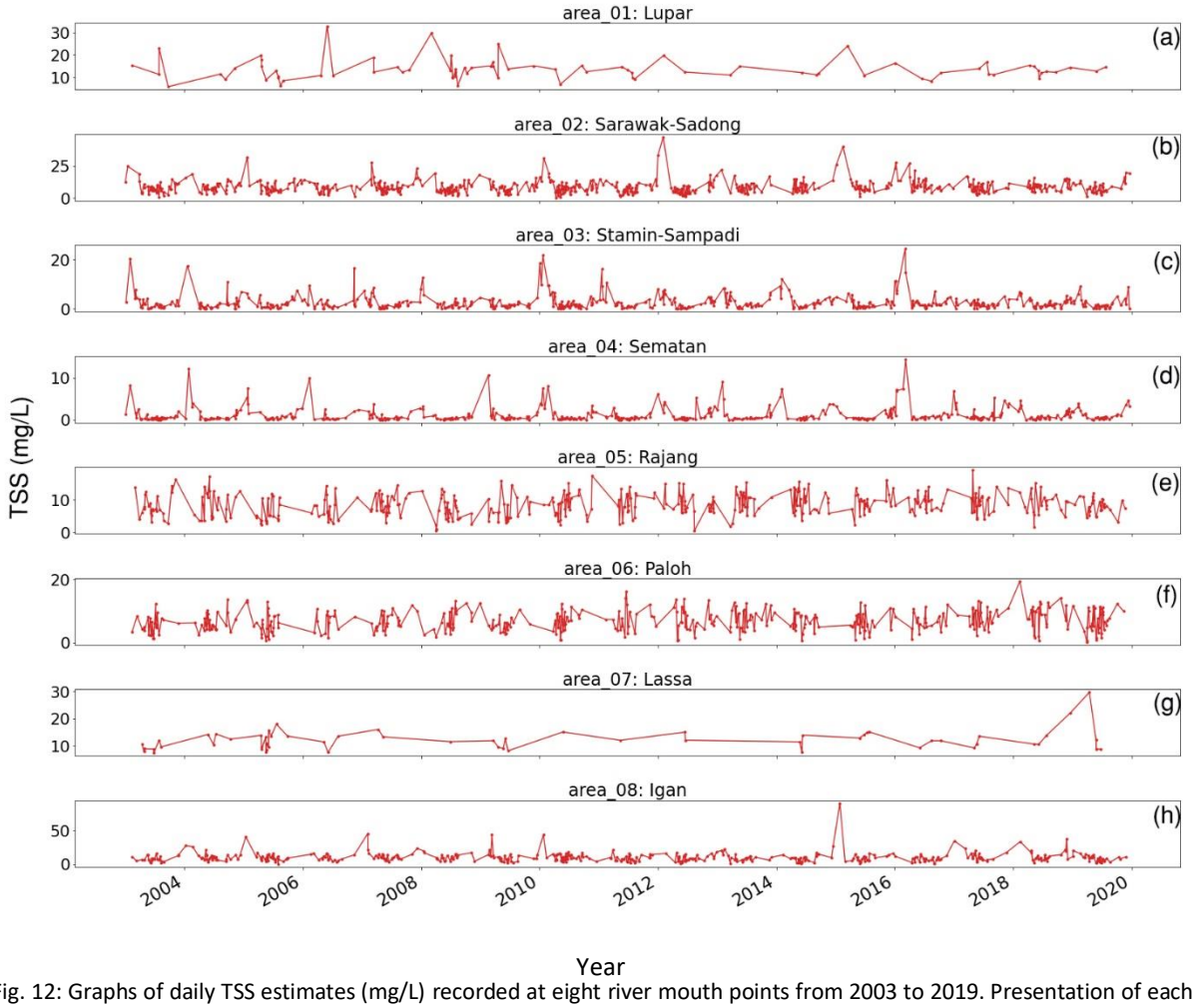

Fig. 12: Graphs of daily TSS estimates (mg/L) recorded at eight river mouth points from 2003 to 2019. Presentation of each river mouths is as follows: a) area_01; b) area_02; c) area_03; d) area_04; e) area_05; f) area_06; g) area_07; h) area_08. Note the different TSS scales in each plot.

From the high temporal resolution graphs in Fig. 12, no general trend of TSS concentration can be identified over the years at each coastal point. It is worth highlighting that the daily temporal resolution was particularly affected at coastal points located in front of the Lupar (area_01) and Lassa (area_07) river mouths due to various pixel data quality issues in these areas. Nonetheless, more than 80 satellite images with minimum cloud coverage at these two locations were processed, while the remaining coastal points had a total of more than 400 satellite images to assess the temporal trend.

549 Despite the fact that no distinct upward or downward trend was observed, our findings indicate that
550 several river mouths are actively discharging and accumulating substantial TSS amounts over the
551 period of years, while resuspension of bottom sediments induced by wind and tidal cycle is another
552 factor contributing to the variation of TSS values (Park, 2007; Song et al., 2020).

553 The coastal region of the Sarawak-Sadong river (area_02) shows relatively high TSS distribution
554 patterns with some periods recording an estimate of over 30 mg/L of TSS concentration. This is in
555 agreement with the localised characteristics of the Sarawak river basin which essentially drains
556 through the populated Kuching area with high industrial and development activities in the capital city
557 of Sarawak (DID, 2021b). In comparison with other river mouth points, a steady TSS concentration
558 below 20 mg/L was recorded across the Stamin-Sampadi (area_03), Sematan (area_04), Rajang
559 (area_05), and Paloh (area_06) river mouths. Consistently high TSS values in the daily plots were
560 recorded at the Lupar (area_01) and Pulau Bruit-Lassa (area_07) river mouths, with estimates of up to
561 30 mg/L on a near-daily basis. Similar high TSS amounts from the Igan (area_08) river mouth, situated
562 northeast side of the Pulau Bruit-Lassa region, were observed in Cherukuru et al. (2021) and Staub et
563 al. (2000).

564 Although the daily TSS estimates at each river point are in line with various reported studies (Chen et
565 al., 2011, 2015b; Kim et al., 2017; Mengen et al., 2020; Zhang et al., 2010a), these estimates can be
566 expected to be much higher for sampling points much closer to the river mouths. The selection of
567 coastal river points in this study was made to minimize the gaps with respect to various pixel data
568 quality issues in the MODIS-Aqua datasets, and hence, the use of coastal river points closer to shore
569 would have been impractical.

570 These findings further suggest that higher TSS loadings within the coastal river areas would have been
571 diluted or deposited while travelling to the open oceanic systems as they are weakly impacted by river
572 discharge in relation to offshore distance (Espinoza Villar et al., 2013). This understanding can be
573 observed in Fig. 13, which shows a progressively decreasing TSS estimates at each transect in relation

574 to the distance from the shore. Generally, TSS estimates in coastal zones (first transect point) show
575 considerably higher TSS concentrations. When moving outwards to territorial waters (second transect
576 point), TSS concentration estimates decrease by nearly 50 % before travelling to open ocean systems
577 (third transect point), except for the northeast regions (area_07 and area_08) which seem to show
578 large extension of TSS plumes to the open ocean waters, as also highlighted by Cherukuru et al. (2021).
579 A reversed trend can be seen in the plot corresponding to the Sematan coastal river systems, although
580 the absolute increase in TSS estimates across water zones (0.2 mg/L in total) here is only marginal (Fig.
581 13d).
582
583
584
585
586

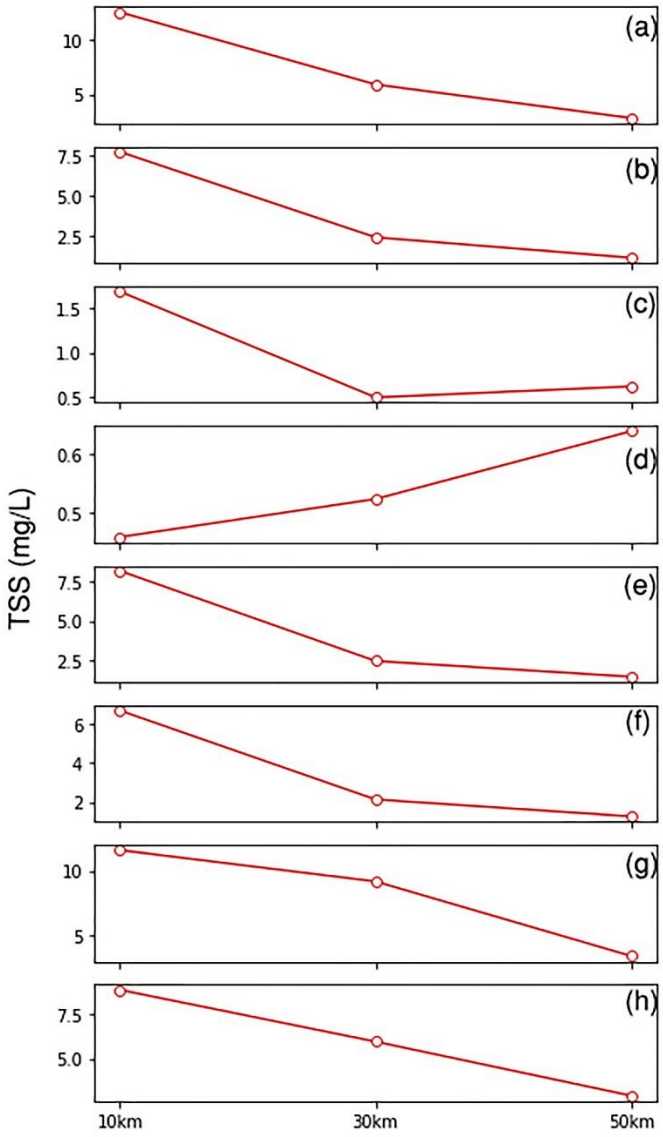

587

588 Fig. 13: Average TSS estimates (mg/L) computed from 2003 to 2019 for each of the eight rivers (area_01: (a), area_02: (b);
589 area_03: (c); area_04: (d); area_05: (e); area_06: (f); area_07: (g); and area_08: (h)) and their relevant transect points with
590 distance of 10 km (coastal waters), 30 km (territorial waters) and 50 km (open ocean waters) from the shoreline. Note the
591 varying TSS scales on the ordinate axes in each plot.

592

593

594

595

3.5 Discussion of TSS implications for coastal waters

High discharge of TSS into coastal environments can lead to adverse environmental and ecological implications. The presence of TSS affects water transparency and light availability within the surface waters (Dogliotti et al., 2015; Nazirova et al., 2021; Wang et al., 2021). Among others, TSS affects the photosynthesis activities of algae and macrophytes. TSS in water creates a reduction in light penetration, which impacts the primary production of aquatic organisms and hence the support system of marine life (Bilotta and Brazier, 2008; Loisel et al., 2014).

Additionally, TSS exerts an influence on zooplankton communities. Reduction in water clarity induces changes in the zooplankton's biomass volume and composition, while TSS may carry a level of toxicity which affects zooplankton through ingestion (Chapman et al., 2017; Donohue and Garcia Molinos, 2009). Apart from that, accumulation and deposition of sediments decreases the level of dissolved oxygen (DO) at the bottom of the water column, and subsequently impacts the benthic invertebrate groups (Chapman et al., 2017). Moreover, substantial TSS deposition tends to cause harmful physical effects to these benthic groups, such as abrasion, and even clogging by sediment particles (Chapman et al., 2017; Langer, 1980).

As a result of these TSS effects on lower trophic levels, fish communities are critically impacted, with a reduction in diversity and abundance (Kemp et al., 2011). While fish communities learn to adapt to a range of TSS loads (Macklin et al., 2010), increase of TSS concentrations often depletes DO concentrations in the water system and causes stress towards these aquatic communities (Henley et al., 2000). Fish populations tend to decrease, as feeding and growth rates are negatively impacted (Shaw and Richardson, 2001; Sutherland and Meyer, 2007).

Threats to coral reefs have been linked to sediment-induced stress which often leads to a reduction in the coral's growth and metabolic rate, as well as impending mortality (Erftemeijer et al., 2012; Gilmour et al., 2006; Risk and Edinger, 2011). Factors of coral stress are driven by nutrient-rich sediments and microbes which are being carried by TSS, with impacts on the health of coral tissues

(Hodgson, 1990; Risk and Edinger, 2011; Weber et al., 2006). A reduction in light availability impedes the development of corals (Anthony and Hoegh-Guldberg, 2003; Rogers, 1979; Telesnicki and Goldberg, 1995). A combined increase in TSS and nutrient loadings contribute to the decrease of coral species diversity and composition (Fabricius, 2005).

Essentially, presence of TSS in water systems has impacts across various aquatic biota. With the severe implications of decreased fish population, this could lead to a disruption of fisheries activities by local communities, especially considering that more than 80 % of the Sarawak population is living in the coastal areas (DID, 2021a). Coral reefs are important coastal biodiversity assets to the Sarawak region, especially around the Talang-Talang and Satang islands on the southwest coast of Sarawak (Long, 2014). With the use of remote sensing technologies in monitoring Sarawak coastal water quality, the approach presented in this paper provides digital-based solutions to assist relevant authorities and local agencies to better manage the Sarawak coastal waters and their resources.

4.0 Conclusion

In this study, a regional empirical TSS retrieval model was developed to analyse TSS dynamics along the southwest coast of Sarawak. The empirical relationship between in situ reflectance values, Rrs(λ), and in situ TSS concentrations was established using a green-to-red band ratio using the MODIS-Aqua Rrs(530) and Rrs(666) reflectance bands. An evaluation of the TSS retrieval model was carried out with error metric assessment, which yielded results of bias = 1.0, MAE = 1.47 and RMSE = 0.22 in mg/L computed in log10-transformed space prior to calculation. A statistical analysis using a k-fold cross validation technique (k = 7) reported low error metrics (RMSE = 0.2159, MAE = 0.1747).

The spatial TSS distribution map shows widespread TSS plumes detected particularly in the Lupar and Rajang coastal areas, with average TSS range of 15 – 20 mg/L estimated at these coastal areas. Based on the spatial map of the TSS coefficient of variation, large TSS variability was identified in the Samunsam-Sematan coastal areas (CV > 90 %). The map of temporal variation of TSS distribution points to a strong monsoonal influence in driving TSS release, with large differences identified

between the northeast and southwest monsoon periods in this region. From the annual TSS anomalies maps, the Samunsam-Sematan coastal areas demonstrated strong TSS variation spatially, while widespread TSS distribution with nearly 100 % of TSS increase in comparison to long term mean was observed in 2010. Furthermore, our study on river discharge in relation to TSS release demonstrated a weak relationship at both the Lupar and Rajang coastal river points. Study on the TSS variability across coastal river mouths implied that higher TSS loadings in the coastal areas are potentially being deposited or diluted in the process of being transported into the open ocean waters, with varying magnitude at several coastal river points.

Overall, these coastal areas of Sarawak are dominantly categorised as Class I quality, which remain within local quality standards to support various marine and socio-economic activities in this region. Our findings in the southwest coastal areas (Sematan and Stamin-Sampadi) showed that the coral reefs there can be well-maintained with negligible impacts from TSS loadings. However, it is important to highlight the various human activities that are widely ongoing in this region, which include deforestation and logging activities (Alamgir et al., 2020; Hon and Shibata, 2013; Vijith et al., 2018). Impacts from these activities in Sarawak can potentially aggravate current soil erosion issues, and ultimately induce more soil leaching and runoff from land to water systems, especially during heavy rainfall events (Ling et al., 2016; Vijith et al., 2018). As a result, human activities may have a greater influence on driving riverine sediments than climatological factors, as reported by Song et al. (2016). As such, this work presents the first observation of TSS distributions at large spatial and temporal scales in Sarawak's coastal systems, and of the potential associated impacts on the South China Sea. The findings derived from this work can be used to support local authorities in assessing TSS water quality status in the coastal areas of concern, and to enhance coastal management and conservation strategies. The application of remote sensing technologies is of great benefit in the development of sustainable sediment management in the Sarawak coastal region, as demonstrated in this study.

Data availability. The dataset related to this study is available as supplement to this paper.

Author contributions. Conceptualization, J.C., N.C., E.L., and M.M.; Formal analysis, J.C., N.C. and E.L.; Funding acquisition, M.M, N.C., and A.M.; Investigation, J.C., N.C., E.L., M.P., P.M., A.M., and M.M.; Methodology, J.C., N.C., E.L., and M.M.; Resources, J.C., N.C., E.L., M.P., and M.M.; Validation, J.C., N.C., E.L. and M.M.; Writing— original draft, J.C..; Writing—review & editing, J.C., N.C., E.L., P.M., and M.M.; Supervision, M.M., N.C., and A.M.; Project administration, M.M., A.M., and N.C.

Competing interests. The authors declare that they have no conflict of interest.

Acknowledgement. We thank Sarawak Forestry Department and Sarawak Biodiversity Centre for permission to conduct collaborative research in Sarawak under permit numbers NPW.907.4.4(Jld.14)-161, SBC-RA-0097-MM, and Park Permit WL83/2017. We would like to extend our gratitude to all the boatmen and crew during all the field expeditions. Special thanks to Pak Mat and Minhad during the western region sampling, and Captain Juble, as well as Lukas Chin, during the eastern region cruises. We are appreciative to members of AQUES MY for their kind participation and involvement, especially to Ashleen Tan, Jack Sim, Florina Richard, Faith Chaya, Edwin Sia, Faddrine Jang, Gonzalo Carrasco, Akhmetzada Kargazhanov, Noor Iskandar Noor Azhar, and Fakharuddin Muhamad. The study was supported by Australian Academy of Sciences under the Regional Collaborations Programme, Sarawak Multimedia Authority (Sarawak Digital Centre of Excellence) and Swinburne University of Technology (Swinburne Research Studentship).

References:

Ahn, Y. and Shanmugam, P.: Derivation and analysis of the fluorescence algorithms to estimate phytoplankton pigment concentrations in optically, , doi:10.1088/1464-4258/9/4/008, 2007.

Alamgir, M., Campbell, M. J., Sloan, S., Engert, J., Word, J. and Laurance, W. F.: Emerging challenges for sustainable development and forest conservation in Sarawak, Borneo, PLoS One, 15(3), 1–20, doi:10.1371/journal.pone.0229614, 2020.

Alcântara, E., Bernardo, N., Watanabe, F., Rodrigues, T., Rotta, L., Carmo, A., Shimabukuro, M., Gonçalves, S. and Imai, N.: Estimating the CDOM absorption coefficient in tropical inland waters using OLI/Landsat-8 images, Remote Sens. Lett., 7(7), 661–670, doi:10.1080/2150704X.2016.1177242, 2016.

Anthony, K. R. N. and Hoegh-Guldberg, O.: Kinetics of photoacclimation in corals, Oecologia, 134(1), 23–31, doi:10.1007/s00442-002-1095-1, 2003.

Babin, M., Stramski, D., Ferrari, G. M., Claustre, H., Bricaud, A., Obolensky, G. and Hoepffner, N.: Variations in the light absorption coefficients of phytoplankton , nonalgal particles , and dissolved organic matter in coastal waters around Europe, , 108, doi:10.1029/2001JC000882, 2003.

Bailey, S. W., Franz, B. A. and Werdell, P. J.: Estimation of near-infrared water-leaving reflectance for satellite ocean color data processing, Opt. Express, 18(7), 7521, doi:10.1364/oe.18.007521, 2010.

Balasubramanian, S. V., Pahlevan, N., Smith, B., Binding, C., Schalles, J., Loisel, H., Gurlin, D., Greb, S., Alikas, K., Randla, M., Bunkei, M., Moses, W., Nguyễn, H., Lehmann, M. K., O'Donnell, D., Ondrusek, M., Han, T. H., Fichot, C. G., Moore, T. and Boss, E.: Robust algorithm for estimating total suspended solids (TSS) in inland and nearshore coastal waters, Remote Sens. Environ., 246(February), 111768, doi:10.1016/j.rse.2020.111768, 2020.

Bhardwaj, J., Gupta, K. K. and Gupta, R.: A review of emerging trends on water quality measurement sensors, Proc. - Int. Conf. Technol. Sustain. Dev. ICTSD 2015, (April), 1–6, doi:10.1109/ICTSD.2015.7095919, 2015.

Bilotta, G. S. and Brazier, R. E.: Understanding the influence of suspended solids on water quality and aquatic biota, Water Res., 42(12), 2849–2861, doi:10.1016/j.watres.2008.03.018, 2008.

Bong, C. H. J. and Richard, J.: Drought and climate change assessment using standardized precipitation index (Spi) for sarawak river basin, J. Water Clim. Chang., 11(4), 956–965, doi:10.2166/wcc.2019.036, 2020.

Cao, F., Tzortziou, M., Hu, C., Mannino, A., Fichot, C. G., Del Vecchio, R., Najjar, R. G. and Novak, M.: Remote sensing retrievals of colored dissolved organic matter and dissolved organic carbon dynamics in North American estuaries and their margins, Remote Sens. Environ., 205(November 2017), 151–165, doi:10.1016/j.rse.2017.11.014, 2018.

Chapman, P. M., Hayward, A. and Faithful, J.: Total Suspended Solids Effects on Freshwater Lake Biota Other than Fish, Bull. Environ. Contam. Toxicol., 99(4), 423–427, doi:10.1007/s00128-017-2154-y, 2017.

Chen, S., Huang, W., Chen, W. and Chen, X.: An enhanced MODIS remote sensing model for detecting rainfall effects on sediment plume in the coastal waters of Apalachicola Bay, Mar. Environ. Res., 72(5), 265–272, doi:10.1016/j.marenvres.2011.09.014, 2011.

Chen, S., Han, L., Chen, X., Li, D., Sun, L. and Li, Y.: Estimating wide range Total Suspended Solids concentrations from MODIS 250-m imageries: An improved method, ISPRS J. Photogramm. Remote Sens., 99, 58–69, doi:10.1016/j.isprsjprs.2014.10.006, 2015a.

Chen, S., Han, L., Chen, X., Li, D., Sun, L. and Li, Y.: Estimating wide range Total Suspended Solids concentrations from MODIS 250-m imageries: An improved method, ISPRS J. Photogramm. Remote Sens., 99, 58–69, doi:10.1016/j.isprsjprs.2014.10.006, 2015b.

Chen, Z., Hu, C. and Muller-karger, F.: Monitoring turbidity in Tampa Bay using MODIS / Aqua 250-m imagery, , 109, 207–220, doi:10.1016/j.rse.2006.12.019, 2007.

Cherukuru, N., Ford, P. W., Matear, R. J., Oubelkheir, K., Clementson, L. A., Suber, K. and Steven, A. D. L.: Estimating dissolved organic carbon concentration in turbid coastal waters using optical remote sensing observations, Int. J. Appl. Earth Obs. Geoinf., 52, 149–154, doi:10.1016/j.jag.2016.06.010, 2016a.

Cherukuru, N., Ford, P. W., Matear, R. J., Oubelkheir, K., Clementson, L. A., Suber, K. and Steven, A. D. L.: Estimating dissolved organic carbon concentration in turbid coastal waters using optical remote sensing observations, Int. J. Appl. Earth Obs. Geoinf., 52, 149–154, doi:10.1016/j.jag.2016.06.010, 2016b.

Cherukuru, N., Martin, P., Sanwlani, N., Mujahid, A. and Müller, M.: A semi-analytical optical remote sensing model to estimate suspended sediment and dissolved organic carbon in tropical coastal waters influenced by peatland-draining river discharges off sarawak, borneo, Remote Sens., 13(1), 1–31, doi:10.3390/rs13010099, 2021.

Chong, X. Y., Gibbins, C. N., Vericat, D., Batalla, R. J., Teo, F. Y. and Lee, K. S. P.: A framework for Hydrological characterisation to support Functional Flows (HyFFlow): Application to a tropical river, J. Hydrol. Reg. Stud., 36(January), doi:10.1016/j.ejrh.2021.100838, 2021.

CIFOR: Forest Carbon Database, [online] Available from: https://carbonstock.cifor.org/, n.d.

Davies, J., Mathhew, U., Aikanathan, S., Nyon, Y. C. and Chong, G.: A Quick Scan of Peatlands, Wetl. Int. Malaysia, 1(March), 1–80, 2010.

Department of Environment: Malaysia Marine Water Quality Standards and Index, , 16 [online] Available from: https://www.doe.gov.my/portalv1/wp-content/uploads/2019/04/BOOKLET-BI.pdf (Accessed 12 September 2021), 2019.

Department of Statistics, M.: Sarawak Population, Popul. by Adm. Dist. Ethn. group, Sarawak, 2020 [online] Available from: https://sarawak.gov.my/web/home/article_view/240/175, 2020.

DID: Department of Irrigation & Drainage Sarawak: Introduction to Integrated Coastal Zone Management, [online] Available from: https://did.sarawak.gov.my/page-0-123-476-INTEGRATED-COASTAL-ZONE-MANAGEMENT.html (Accessed 21 October 2021a), 2021.

DID: Department Of Irrigation & Drainage Sarawak, 2021b.

Dindang, A., Chung, C. N. and Seth, S.: Heavy Rainfall Episodes over Sarawak during January-February 2011 Northeast Monsoon, JMM Res. Publ., (11), 41, 2011.

Dogliotti, A. I., Ruddick, K. G., Nechad, B., Doxaran, D. and Knaeps, E.: A single algorithm to retrieve turbidity from remotely-sensed data in all coastal and estuarine waters, Remote Sens. Environ., 156, 157–168, doi:10.1016/j.rse.2014.09.020, 2015.

Donohue, I. and Garcia Molinos, J.: Impacts of increased sediment loads on the ecology of lakes, Biol. Rev., 84(4), 517–531, doi:10.1111/j.1469-185X.2009.00081.x, 2009.

Erftemeijer, P. L. A., Riegl, B., Hoeksema, B. W. and Todd, P. A.: Environmental impacts of dredging and other sediment disturbances on corals: A review, Mar. Pollut. Bull., 64(9), 1737–1765, doi:10.1016/j.marpolbul.2012.05.008, 2012.

Espinoza Villar, R., Martinez, J. M., Le Texier, M., Guyot, J. L., Fraizy, P., Meneses, P. R. and Oliveira, E. de: A study of sediment transport in the Madeira River, Brazil, using MODIS remote-sensing images, J. South Am. Earth Sci., 44, 45–54, doi:10.1016/j.jsames.2012.11.006, 2013.

Fabricius, K. E.: Effects of terrestrial runoff on the ecology of corals and coral reefs: Review and synthesis, Mar. Pollut. Bull., 50(2), 125–146, doi:10.1016/j.marpolbul.2004.11.028, 2005.

Fabricius, K. E., Logan, M., Weeks, S. J., Lewis, S. E. and Brodie, J.: Changes in water clarity in response to river discharges on the Great Barrier Reef continental shelf: 2002-2013, Estuar. Coast. Shelf Sci., 173, A1–A15, doi:10.1016/j.ecss.2016.03.001, 2016.

Gaveau, D. L. A., Sheil, D., Salim, M. A., Arjasakusuma, S., Ancrenaz, M., Pacheco, P. and Meijaard, E.: Rapid conversions and avoided deforestation : examining four decades of industrial plantation expansion in Borneo, Nat. Publ. Gr., (September), 1–13, doi:10.1038/srep32017, 2016.

Gilmour, J. P., Cooper, T. F., Fabricius, K. E. and Smith, L. D.: Early warning indicators of change in the condition of corals and coral communities in response to key anthropogenic stressors in the Pilbara, Western Australia, Aust. Inst. Mar. Sci. Rep. to Environ. Prot. Authority. 101pp, 2006.

Giuliani, G., Chatenoux, B., Piller, T., Moser, F. and Lacroix, P.: Data Cube on Demand (DCoD): Generating an earth observation Data Cube anywhere in the world, Int. J. Appl. Earth Obs. Geoinf., 87(December 2019), 102035, doi:10.1016/j.jag.2019.102035, 2020.

Gomes, V. C. F., Carlos, F. M., Queiroz, G. R., Ferreira, K. R. and Santos, R.: Accessing and Processing Brazilian Earth Observation Data Cubes With the Open Data Cube Platform, ISPRS Ann. Photogramm. Remote Sens. Spat. Inf. Sci., V-4–2021, 153–159, doi:10.5194/isprs-annals-v-4-2021-153-2021, 2021.

Gomyo, M. and Koichiro, K.: Spatial and temporal variations in rainfall and the ENSO-rainfall relationship over Sarawak, Malaysian Borneo, Sci. Online Lett. Atmos., 5, 41–44, doi:10.2151/sola.2009-011, 2009.

González Vilas, L., Spyrakos, E. and Torres Palenzuela, J. M.: Neural network estimation of chlorophyll a from MERIS full resolution data for the coastal waters of Galician rias (NW Spain), Remote Sens. Environ., 115(2), 524–535, doi:10.1016/j.rse.2010.09.021, 2011.

Ha, N. T. T., Thao, N. T. P., Koike, K. and Nhuan, M. T.: Selecting the best band ratio to estimate chlorophyll-a concentration in a tropical freshwater lake using sentinel 2A images from a case study of Lake Ba Be (Northern Vietnam), ISPRS Int. J. Geo-Information, 6(9), doi:10.3390/ijgi6090290, 2017.

Henley, W. F., Patterson, M. A., Neves, R. J. and Dennis Lemly, A.: Effects of Sedimentation and Turbidity on Lotic Food Webs: A Concise Review for Natural Resource Managers, Rev. Fish. Sci., 8(2), 125–139, doi:10.1080/10641260091129198, 2000.

Hodgson, G.: Tetracycline reduces sedimentation damage to corals, Mar. Biol., 104(3), 493–496, 1990.

Hon, J. and Shibata, S.: A Review on Land Use in the Malaysian State of Sarawak, Borneo and Recommendations for Wildlife Conservation Inside Production Forest Environment, Borneo J. Resour. Sci. Technol., 3(2), 22–35, doi:10.33736/bjrst.244.2013, 2013.

Horsburgh, J. S., Spackman, A., Stevens, D. K., Tarboton, D. G. and Mesner, N. O.: Environmental Modelling & Software A sensor network for high frequency estimation of water quality constituent fluxes using surrogates, , 25, 1031–1044, doi:10.1016/j.envsoft.2009.10.012, 2010.

Howarth, R. W.: Coastal nitrogen pollution: A review of sources and trends globally and regionally, Harmful Algae, 8(1), 14–20, doi:10.1016/j.hal.2008.08.015, 2008.

825 Hu, C., Lee, Z. and Franz, B.: Chlorophyll a algorithms for oligotrophic oceans: A novel approach
826 based on three-band reflectance difference, J. Geophys. Res. Ocean., 117(1), 1–25,
827 doi:10.1029/2011JC007395, 2012.

828 Jiang, D., Matsushita, B., Pahlevan, N., Gurlin, D., Lehmann, M. K., Fichot, C. G., Schalles, J., Loisel, H.,
829 Binding, C., Zhang, Y., Alikas, K., Kangro, K., Uusõue, M., Ondrusek, M., Greb, S., Moses, W. J.,
830 Lohrenz, S. and O'Donnell, D.: Remotely estimating total suspended solids concentration in clear to
831 extremely turbid waters using a novel semi-analytical method, Remote Sens. Environ., 258,
832 doi:10.1016/j.rse.2021.112386, 2021.

833 Jiang, H. and Liu, Y.: Monitoring of TSS concentration in Poyang Lake based on MODIS data, Yangtze
834 River, 42(17), 87–90, 2011.

835 Kemp, P., Sear, D., Collins, A., Naden, P. and Jones, I.: The impacts of fine sediment on riverine fish,
836 Hydrol. Process., 25(11), 1800–1821, doi:10.1002/hyp.7940, 2011.

837 Killough, B.: The Impact of Analysis Ready Data in the Africa Regional Data Cube, Int. Geosci. Remote
838 Sens. Symp., (July 2019), 5646–5649, doi:10.1109/IGARSS.2019.8898321, 2019.

839 Kim, H. C., Son, S., Kim, Y. H., Khim, J. S., Nam, J., Chang, W. K., Lee, J. H., Lee, C. H. and Ryu, J.:
840 Remote sensing and water quality indicators in the Korean West coast: Spatio-temporal structures of
841 MODIS-derived chlorophyll-a and total suspended solids, Mar. Pollut. Bull., 121(1–2), 425–434,
842 doi:10.1016/j.marpolbul.2017.05.026, 2017.

843 Krause, C., Dunn, B., Bishop-Taylor, R., Adams, C., Burton, C., Alger, M., Chua, S., Phillips, C., Newey,
844 V., Kouzoubov, K., Leith, A., Ayers, D., Hicks, A. and DEA Notebooks contributors 2021: Digital Earth
845 Australia notebooks and tools repository, , doi:https://doi.org/10.26186/145234, 2021.

846 Kuok, K. K., Chiu, P., Yap, A. and Law, K.: Determination of the Best Tank Model for the Southern
847 Region of Sarawak Determination Number of Tanks for Tank Model at Southern Region of Sarawak, ,
848 (August 2012), 2018.

849 Langer, O. E.: Effects of sedimentation on salmonid stream life, Environmental Protection Service.,
850 1980.

851 Lavigne, H., Van der Zande, D., Ruddick, K., Cardoso Dos Santos, J. F., Gohin, F., Brotas, V. and
852 Kratzer, S.: Quality-control tests for OC4, OC5 and NIR-red satellite chlorophyll-a algorithms applied
853 to coastal waters, Remote Sens. Environ., 255, 112237, doi:10.1016/j.rse.2020.112237, 2021.

854 Lee, K. H., Noh, J. and Khim, J. S.: The Blue Economy and the United Nations' sustainable
855 development goals: Challenges and opportunities, Environ. Int., 137(October 2019), 105528,
856 doi:10.1016/j.envint.2020.105528, 2020a.

857 Lee, W. C., Viswanathan, K. K., Kamri, T. and King, S.: Status of Sarawak Fisheries: Challenges and
858 Way Forward, Int. J. Serv. Manag. Sustain., 5(2), 187–200, doi:10.24191/ijsms.v5i2.11719, 2020b.

859 Lehner, B., Verdin, K. and Jarvis, A.: HydroSHEDS technical documentation, World Wildl. Fund US,
860 Washington, DC, 1–27, 2006.

861 Lemley, D. A., Adams, J. B., Bornman, T. G., Campbell, E. E. and Deyzel, S. H. P.: Land-derived
862 inorganic nutrient loading to coastal waters and potential implications for nearshore plankton
863 dynamics, Cont. Shelf Res., 174(August 2018), 1–11, doi:10.1016/j.csr.2019.01.003, 2019.

864 Lewis, A., Oliver, S., Lymburner, L., Evans, B., Wyborn, L., Mueller, N., Raevksi, G., Hooke, J.,
865 Woodcock, R., Sixsmith, J., Wu, W., Tan, P., Li, F., Killough, B., Minchin, S., Roberts, D., Ayers, D.,
866 Bala, B., Dwyer, J., Dekker, A., Dhu, T., Hicks, A., Ip, A., Purss, M., Richards, C., Sagar, S., Trenham, C.,
867 Wang, P. and Wang, L. W.: The Australian Geoscience Data Cube — Foundations and lessons

868 learned, Remote Sens. Environ., 202, 276–292, doi:10.1016/j.rse.2017.03.015, 2017.

869 Limcih, F., Jilnm, M., Hb, H., Ilcach, H. N. M., Mnl, F., Fi, F. and Nb, F.: Study of Coastal Areas in Miri,
870 in World Engineering Congress 2010, pp. 56–65., 2010.

871 Ling, T. Y., Soo, C. L., Sivalingam, J. R., Nyanti, L., Sim, S. F. and Grinang, J.: Assessment of the Water
872 and Sediment Quality of Tropical Forest Streams in Upper Reaches of the Baleh River, Sarawak,
873 Malaysia, Subjected to Logging Activities, J. Chem., 2016, doi:10.1155/2016/8503931, 2016.

874 Liu, B., D'Sa, E. J. and Joshi, I.: Multi-decadal trends and influences on dissolved organic carbon
875 distribution in the Barataria Basin, Louisiana from in-situ and Landsat/MODIS observations, Remote
876 Sens. Environ., 228(May), 183–202, doi:10.1016/j.rse.2019.04.023, 2019.

877 Loisel, H., Mangin, A., Vantrepotte, V., Dessailly, D., Ngoc Dinh, D., Garnesson, P., Ouillon, S.,
878 Lefebvre, J. P., Mériaux, X. and Minh Phan, T.: Variability of suspended particulate matter
879 concentration in coastal waters under the Mekong's influence from ocean color (MERIS) remote
880 sensing over the last decade, Remote Sens. Environ., 150, 218–230, doi:10.1016/j.rse.2014.05.006,
881 2014.

882 Long, S. M.: Sarawak Coastal Biodiversity : A Current Status, Kuroshio Sci., 8(1), 71–84 [online]
883 Available from: https://www.researchgate.net/publication/265793245, 2014.

884 Lu, Y., Yuan, J., Lu, X., Su, C., Zhang, Y., Wang, C., Cao, X., Li, Q., Su, J., Ittekkot, V., Garbutt, R. A.,
885 Bush, S., Fletcher, S., Wagey, T., Kachur, A. and Sweijd, N.: Major threats of pollution and climate
886 change to global coastal ecosystems and enhanced management for sustainability, Environ. Pollut.,
887 239, 670–680, doi:10.1016/j.envpol.2018.04.016, 2018.

888 Macklin, M. G., Jones, A. F. and Lewin, J.: River response to rapid Holocene environmental change:
889 evidence and explanation in British catchments, Quat. Sci. Rev., 29(13–14), 1555–1576,
890 doi:10.1016/j.quascirev.2009.06.010, 2010.

891 Mao, Z., Chen, J., Pan, D., Tao, B. and Zhu, Q.: A regional remote sensing algorithm for total
892 suspended matter in the East China Sea, Remote Sens. Environ., 124, 819–831,
893 doi:10.1016/j.rse.2012.06.014, 2012.

894 Martin, P., Cherukuru, N., Tan, A. S. Y., Sanwlani, N., Mujahid, A. and Müller, M.: Distribution and
895 cycling of terrigenous dissolved organic carbon in peatland-draining rivers and coastal waters of
896 Sarawak, Borneo, Biogeosciences, 15(22), 6847–6865, doi:10.5194/bg-15-6847-2018, 2018.

897 Mengen, D., Ottinger, M., Leinenkugel, P. and Ribbe, L.: Modeling river discharge using automated
898 river width measurements derived from sentinel-1 time series, Remote Sens., 12(19), 1–24,
899 doi:10.3390/rs12193236, 2020.

900 Milliman, J. D. and Farnsworth, K. L.: River discharge to the coastal ocean: a global synthesis,
901 Cambridge University Press., 2013.

902 Mohammad Razi, M. A., Mokhtar, A., Mahamud, M., Rahmat, S. N. and Al-Gheethi, A.: Monitoring of
903 river and marine water quality at Sarawak baseline, Environ. Forensics, 22(1–2), 219–240,
904 doi:10.1080/15275922.2020.1836076, 2021.

905 Morel, A. and Bélanger, S.: Improved detection of turbid waters from ocean color sensors
906 information, Remote Sens. Environ., 102(3–4), 237–249, doi:10.1016/j.rse.2006.01.022, 2006.

907 Morel, A. and Gentili, B.: A simple band ratio technique to quantify the colored dissolved and detrital
908 organic material from ocean color remotely sensed data, Remote Sens. Environ., 113(5), 998–1011,
909 doi:10.1016/j.rse.2009.01.008, 2009.

910 Mueller, J., Muellıer, J., Pietras, C., Hooker, S., Clark, D., Frouin, A., Mitchell, B., Bidigare, R., Trees, C.

911 and Werdell, J.: Ocean Optics Protocols For Satellite Ocean Color Sensor Validation, Revision 3,
912 volumes 1 and 2., 2002.

913 Müller-dum, D., Warneke, T., Rixen, T., Müller, M., Baum, A., Christodoulou, A., Oakes, J., Eyre, B. D.
914 and Notholt, J.: Impact of peatlands on carbon dioxide (CO 2) emissions from the Rajang River and
915 Estuary , Malaysia, , 17–32, 2019.

916 Müller, D., Warneke, T., Rixen, T., Müller, M., Mujahid, A., Bange, H. W. and Notholt, J.: Fate of
917 terrestrial organic carbon and associated CO2 and CO emissions from two Southeast Asian estuaries,
918 Biogeosciences, 13(3), 691–705, doi:10.5194/bg-13-691-2016, 2016.

919 NASA Official: Ocean Level-2 Data Format Specification, [online] Available from:
920 https://oceancolor.gsfc.nasa.gov/docs/format/l2nc/, n.d.

921 Nazirova, K., Alferyeva, Y., Lavrova, O., Shur, Y., Soloviev, D., Bocharova, T. and Strochkov, A.:
922 Comparison of in situ and remote-sensing methods to determine turbidity and concentration of
923 suspended matter in the estuary zone of the mzymta river, black sea, Remote Sens., 13(1), 1–29,
924 doi:10.3390/rs13010143, 2021.

925 Neil, C., Spyrakos, E., Hunter, P. D. and Tyler, A. N.: A global approach for chlorophyll-a retrieval
926 across optically complex inland waters based on optical water types, Remote Sens. Environ.,
927 229(May), 159–178, doi:10.1016/j.rse.2019.04.027, 2019.

928 Ondrusek, M., Stengel, E., Kinkade, C. S., Vogel, R. L., Keegstra, P., Hunter, C. and Kim, C.: The
929 development of a new optical total suspended matter algorithm for the Chesapeake Bay, Remote
930 Sens. Environ., 119, 243–254, doi:10.1016/j.rse.2011.12.018, 2012.

931 Open Data Cube: Open Data Cube, [online] Available from:
932 https://opendatacube.readthedocs.io/en/latest/user/intro.html (Accessed 25 October 2021), 2021.

933 Park, G. S.: The role and distribution of total suspended solids in the macrotidal coastal waters of
934 Korea, Environ. Monit. Assess., 135(1–3), 153–162, doi:10.1007/s10661-007-9640-3, 2007.

935 Petus, C., Marieu, V., Novoa, S., Chust, G., Bruneau, N. and Froidefond, J. M.: Monitoring spatio-
936 temporal variability of the Adour River turbid plume (Bay of Biscay, France) with MODIS 250-m
937 imagery, Cont. Shelf Res., 74, 35–49, doi:10.1016/j.csr.2013.11.011, 2014.

938 Praveena, S. M., Siraj, S. S. and Aris, A. Z.: Coral reefs studies and threats in Malaysia: A mini review,
939 Rev. Environ. Sci. Biotechnol., 11(1), 27–39, doi:10.1007/s11157-011-9261-8, 2012.

940 Ramaswamy, V., Rao, P. S., Rao, K. H., Thwin, S., Rao, N. S. and Raiker, V.: Tidal influence on
941 suspended sediment distribution and dispersal in the northern Andaman Sea and Gulf of Martaban,
942 Mar. Geol., 208(1), 33–42, doi:10.1016/j.margeo.2004.04.019, 2004.

943 Refaeilzadeh, P., Tang, L., Liu, H., Angeles, L. and Scientist, C. D.: Encyclopedia of Database Systems,
944 Encycl. Database Syst., doi:10.1007/978-1-4899-7993-3, 2020.

945 Risk, M. J. and Edinger, E.: Impacts of sediment on coral reefs, Encycl. Mod. coral reefs. Springer,
946 Netherlands, 575–586, 2011.

947 Rogers, C. S.: The effect of shading on coral reef structure and function, J. Exp. Mar. Bio. Ecol., 41(3),
948 269–288, doi:10.1016/0022-0981(79)90136-9, 1979.

949 Sa'adi, Z., Shahid, S., Chung, E. S. and Ismail, T. bin: Projection of spatial and temporal changes of
950 rainfall in Sarawak of Borneo Island using statistical downscaling of CMIP5 models, Atmos. Res.,
951 197(November 2016), 446–460, doi:10.1016/j.atmosres.2017.08.002, 2017.

952 Sandifer, P. A., Keener, P., Scott, G. I. and Porter, D. E.: Oceans and Human Health and the New Blue

953 Economy, Elsevier Inc., 2021.

954 Sarawak Forestry Corporation: Maludam National Park, [online] Available from:
955 https://sarawakforestry.com/parks-and-reserves/maludam-national-park/, 2022.

956 Seegers, B. N., Stumpf, R. P., Schaeffer, B. A., Loftin, K. A. and Werdell, P. J.: Performance metrics for
957 the assessment of satellite data products: an ocean color case study, Opt. Express, 26(6), 7404,
958 doi:10.1364/oe.26.007404, 2018.

959 Shaw, E. Al and Richardson, J. S.: Direct and indirect effects of sediment pulse duration on stream
960 invertebrate assemblages and rainbow trout (Oncorhynchus mykiss) growth and survival, Can. J.
961 Fish. Aquat. Sci., 58(11), 2213–2221, doi:10.1139/f01-160, 2001.

962 Sim, C., Cherukuru, N., Mujahid, A., Martin, P., Sanwlani, N., Warneke, T., Rixen, T., Notholt, J. and
963 Müller, M.: A new remote sensing method to estimate river to ocean DOC flux in peatland
964 dominated Sarawak coastal regions, Borneo, Remote Sens., 12(20), 1–13, doi:10.3390/rs12203380,
965 2020.

966 Siswanto, E., Tang, J. and Yamaguchi, H.: Empirical ocean-color algorithms to retrieve chlorophyll- a ,
967 total suspended matter , and colored dissolved organic matter absorption coefficient in the Yellow
968 and East China Seas, , 627–650, doi:10.1007/s10872-011-0062-z, 2011.

969 Slonecker, E. T., Jones, D. K. and Pellerin, B. A.: The new Landsat 8 potential for remote sensing of
970 colored dissolved organic matter (CDOM), Mar. Pollut. Bull., 107(2), 518–527,
971 doi:10.1016/j.marpolbul.2016.02.076, 2016.

972 Song, C., Wang, G., Sun, X., Chang, R. and Mao, T.: Control factors and scale analysis of annual river
973 water, sediments and carbon transport in China, Sci. Rep., 6(May), 1–14, doi:10.1038/srep25963,
974 2016.

975 Song, Z., Shi, W., Zhang, J., Hu, H., Zhang, F. and Xu, X.: Transport mechanism of suspended
976 sediments and migration trends of sediments in the central hangzhou bay, Water (Switzerland),
977 12(8), doi:10.3390/W12082189, 2020.

978 Soo, C. L., Chen, C. A. and Mohd-Long, S.: Assessment of Near-Bottom Water Quality of
979 Southwestern Coast of Sarawak, Borneo, Malaysia: A Multivariate Statistical Approach, J. Chem.,
980 2017, doi:10.1155/2017/1590329, 2017.

981 Soum, S., Ngor, P. B., Dilts, T. E., Lohani, S., Kelson, S., Null, S. E., Tromboni, F., Hogan, Z. S., Chan, B.
982 and Chandra, S.: Spatial and long-term temporal changes in water quality dynamics of the tonle sap
983 ecosystem, Water (Switzerland), 13(15), doi:10.3390/w13152059, 2021.

984 Staub, J. R. and Esterle, J. S.: Provenance and sediment dispersal in the Rajang River delta/coastal
985 plain system, Sarawak, East Malaysia, Sediment. Geol., 85(1–4), 191–201, doi:10.1016/0037-
986 0738(93)90083-H, 1993.

987 Staub, J. R., Among, H. L. and Gastaldo, R. A.: Seasonal sediment transport and deposition in the
988 Rajang River delta, Sarawak, East Malaysia, Sediment. Geol., 133(3–4), 249–264, doi:10.1016/S0037-
989 0738(00)00042-7, 2000.

990 Sun, C.: Riverine influence on ocean color in the equatorial South China Sea, Cont. Shelf Res.,
991 143(December 2015), 151–158, doi:10.1016/j.csr.2016.10.008, 2017a.

992 Sun, C.: Riverine influence on ocean color in the equatorial South China Sea, Cont. Shelf Res.,
993 143(October 2016), 151–158, doi:10.1016/j.csr.2016.10.008, 2017b.

994 Sutherland, A. B. and Meyer, J. L.: Effects of increased suspended sediment on growth rate and gill
995 condition of two southern Appalachian minnows, Environ. Biol. Fishes, 80(4), 389–403,

996 doi:10.1007/s10641-006-9139-8, 2007.

997 Swain, R. and Sahoo, B.: Mapping of heavy metal pollution in river water at daily time-scale using
998 spatio-temporal fusion of MODIS-aqua and Landsat satellite imageries, J. Environ. Manage., 192, 1–
999 14, doi:10.1016/j.jenvman.2017.01.034, 2017.

1000 Tangang, F. T., Juneng, L., Salimun, E., Sei, K. M., Le, L. J. and Muhamad, H.: Climate change and
1001 variability over Malaysia: Gaps in science and research information, Sains Malaysiana, 41(11), 1355–
1002 1366, 2012.

1003 Tawan, A. S., Ling, T. Y., Nyanti, L., Sim, S. F., Grinang, J., Soo, C. L., Lee, K. S. P. and Ganyai, T.:
1004 Assessment of water quality and pollutant loading of the Rajang River and its tributaries at Pelagus
1005 area subjected to seasonal variation and river regulation, Environ. Dev. Sustain., 22(5), 4101–4124,
1006 doi:10.1007/s10668-019-00374-9, 2020.

1007 Telesnicki, G. J. and Goldberg, W. M.: CORAL REEF PAPER EFFECTS OF TURBIDITY ON THE
1008 PHOTOSYNTHESIS AND RESPIRATION OF TWO SOUTH FLORIDA REEF CORAL SPECIES portant factors
1009 in the regulation of coral cover , diversity , and abundance (Ed- ships between suspended sediment
1010 concentrations or parti, , 57(2), 527–539, 1995.

1011 Tilburg, C. E., Jordan, L. M., Carlson, A. E., Zeeman, S. I. and Yund, P. O.: The effects of precipitation,
1012 river discharge, land use and coastal circulation on water quality in coastal Maine, R. Soc. Open Sci.,
1013 2(7), doi:10.1098/rsos.140429, 2015.

1014 Tromboni, F., Dilts, T. E., Null, S. E., Lohani, S., Ngor, P. B., Soum, S., Hogan, Z. and Chandra, S.:
1015 Changing land use and population density are degrading water quality in the lower mekong basin,
1016 Water (Switzerland), 13(14), 1–16, doi:10.3390/w13141948, 2021.

1017 United Nations: The Ocean Conference, in The Ocean Conference, vol. 53, p. 130, New York., 2017.

1018 Valerio, A. de M., Kampel, M., Vantrepotte, V., Ward, N. D., Sawakuchi, H. O., Less, D. F. D. S., Neu,
1019 V., Cunha, A. and Richey, J.: Using CDOM optical properties for estimating DOC concentrations and
1020 pCO 2 in the Lower Amazon River , Opt. Express, 26(14), A657, doi:10.1364/oe.26.00a657, 2018.

1021 Verschelling, E., van der Deijl, E., van der Perk, M., Sloff, K. and Middelkoop, H.: Effects of discharge,
1022 wind, and tide on sedimentation in a recently restored tidal freshwater wetland, Hydrol. Process.,
1023 31(16), 2827–2841, doi:10.1002/hyp.11217, 2017.

1024 Vijith, H., Hurmain, A. and Dodge-Wan, D.: Impacts of land use changes and land cover alteration on
1025 soil erosion rates and vulnerability of tropical mountain ranges in Borneo, Remote Sens. Appl. Soc.
1026 Environ., 12(September), 57–69, doi:10.1016/j.rsase.2018.09.003, 2018.

1027 Wang, C., Chen, S., Li, D., Wang, D., Liu, W. and Yang, J.: A Landsat-based model for retrieving total
1028 suspended solids concentration of estuaries and coasts in China, Geosci. Model Dev., 10(12), 4347–
1029 4365, doi:10.5194/gmd-10-4347-2017, 2017.

1030 Wang, J., Tong, Y., Feng, L., Zhao, D., Zheng, C. and Tang, J.: Satellite-Observed Decreases in Water
1031 Turbidity in the Pearl River Estuary: Potential Linkage With Sea-Level Rise, J. Geophys. Res. Ocean.,
1032 126(4), 1–17, doi:10.1029/2020JC016842, 2021.

1033 Weber, M., Lott, C. and Fabricius, K. E.: Sedimentation stress in a scleractinian coral exposed to
1034 terrestrial and marine sediments with contrasting physical, organic and geochemical properties, J.
1035 Exp. Mar. Bio. Ecol., 336(1), 18–32, doi:10.1016/j.jembe.2006.04.007, 2006.

1036 Werdell, P. J., McKinna, L. I. W., Boss, E., Ackleson, S. G., Craig, S. E., Gregg, W. W., Lee, Z.,
1037 Maritorena, S., Roesler, C. S., Rousseaux, C. S., Stramski, D., Sullivan, J. M., Twardowski, M. S.,
1038 Tzortziou, M. and Zhang, X.: An overview of approaches and challenges for retrieving marine

inherent optical properties from ocean color remote sensing, Prog. Oceanogr., 160, 186–212, doi:10.1016/j.pocean.2018.01.001, 2018.

Whitmore, T. C.: Tropical rain forests of the Par East, Oxford. Clarendon Press., 1984.

Wilber, D. H. and Clarke, D. G.: Biological Effects of Suspended Sediments: A Review of Suspended Sediment Impacts on Fish and Shellfish with Relation to Dredging Activities in Estuaries, North Am. J. Fish. Manag., 21(4), 855–875, doi:10.1577/1548-8675(2001)021<0855:beossa>2.0.co;2, 2001.

World Bank and United Nations Department of Economic and Social Affairs (UNDESA): The Potential of the Blue Economy: Increasing Long-term Benefits of the Sustainable Use of Marine Resources for Small Island Developing States and Coastal Least Developed Countries, World Bank, Washington DC., 2017.

Wu, C. S., Yang, S. L. and Lei, Y. ping: Quantifying the anthropogenic and climatic impacts on water discharge and sediment load in the Pearl River (Zhujiang), China (1954-2009), J. Hydrol., 452–453, 190–204, doi:10.1016/j.jhydrol.2012.05.064, 2012.

Yang, S. L., Zhao, Q. Y. and Belkin, I. M.: Temporal variation in the sediment load of the Yangtze river and the influences of human activities, J. Hydrol., 263(1–4), 56–71, doi:10.1016/S0022-1694(02)00028-8, 2002.

Zhan, W., Wu, J., Wei, X., Tang, S. and Zhan, H.: Spatio-temporal variation of the suspended sediment concentration in the Pearl River Estuary observed by MODIS during 2003–2015, Cont. Shelf Res., 172(May 2018), 22–32, doi:10.1016/j.csr.2018.11.007, 2019.

Zhang, L. J., Wang, L., Cai, W. J., Liu, D. M. and Yu, Z. G.: Impact of human activities on organic carbon transport in the Yellow River, Biogeosciences, 10(4), 2513–2524, doi:10.5194/bg-10-2513-2013, 2013.

Zhang, M., Tang, J., Dong, Q., Song, Q. T. and Ding, J.: Retrieval of total suspended matter concentration in the Yellow and East China Seas from MODIS imagery, Remote Sens. Environ., 114(2), 392–403, doi:10.1016/j.rse.2009.09.016, 2010a.

Zhang, Y., Lin, S., Liu, J., Qian, X. and Ge, Y.: Time-series MODIS image-based retrieval and distribution analysis of total suspended matter concentrations in Lake Taihu (China), Int. J. Environ. Res. Public Health, 7(9), 3545–3560, doi:10.3390/ijerph7093545, 2010b.

Zhou, Y., Xuan, J. and Huang, D.: Tidal variation of total suspended solids over the Yangtze Bank based on the geostationary ocean color imager, Sci. China Earth Sci., 63(9), 1381–1389, doi:10.1007/s11430-019-9618-7, 2020.

1079

1080

1081

1082

1083

1084

1085

1086